

THE GALACTIC DISTRIBUTION OF OB ASSOCIATIONS IN MOLECULAR CLOUDS

JONATHAN P. WILLIAMS

Harvard-Smithsonian Center for Astrophysics, MS 42, 60 Garden Street, Cambridge, MA 02138

AND

CHRISTOPHER F. MCKEE

Departments of Physics and Astronomy, University of California, Berkeley, CA 94720

Received 1995 June 23; accepted 1996 August 20

ABSTRACT

Molecular clouds account for half of the mass of the interstellar medium interior to the solar circle and for all current star formation. Using cloud catalogs of two CO surveys of the first quadrant, we have fitted the mass distribution of molecular clouds to a truncated power law in a similar manner as the luminosity function of OB associations in the companion paper to this work. After extrapolating from the first quadrant to the entire inner Galaxy, we find that the mass of cataloged clouds amounts to only 40% of current estimates of the total Galactic molecular mass. Following Solomon & Rivolo, we have assumed that the remaining molecular gas is in cold clouds, and we normalize the distribution accordingly. The predicted total number of clouds is then shown to be consistent with that observed in the solar neighborhood where cloud catalogs should be more complete. Within the solar circle, the cumulative form of the distribution is $\mathcal{N}_c(>M) = 105[(M_u/M)^{0.6} - 1]$, where \mathcal{N}_c is the number of clouds, and $M_u = 6 \times 10^6 M_\odot$ is the upper mass limit. The large number of clouds near the upper cutoff to the distribution indicates an underlying physical limit to cloud formation or destruction processes. The slope of the distribution corresponds to $d\mathcal{N}_c/dM \propto M^{-1.6}$, implying that although numerically most clouds are of low mass, most of the molecular gas is contained within the most massive clouds.

The distribution of cloud masses is then compared to the Galactic distribution of OB association luminosities to obtain statistical estimates of the number of massive stars expected in any given cloud. The likelihood of massive star formation in a cloud is determined, and it is found that the median cloud mass that contains at least one O star is $\sim 10^5 M_\odot$. The average star formation efficiency over the lifetime of an association is about 5% but varies by more than 2 orders of magnitude from cloud to cloud and is predicted to increase with cloud mass. O stars photoevaporate their surrounding molecular gas, and even with low rates of formation, they are the principal agents of cloud destruction. Using an improved estimate of the timescale for photoevaporation and our statistics on the expected numbers of stars per cloud, we find that $10^6 M_\odot$ giant molecular clouds (GMCs) are expected to survive for about 3×10^7 yr. Smaller clouds are disrupted, rather than photoionized, by photoevaporation. The porosity of H II regions in large GMCs is shown to be of order unity, which is consistent with self-regulation of massive star formation in GMCs. On average, 10% of the mass of a GMC is converted to stars by the time it is destroyed by photoevaporation.

Subject headings: H II regions — ISM: clouds — ISM: molecules —
open clusters and associations: general — stars: formation

1. INTRODUCTION

Molecular gas is the raw material out of which stars are manufactured. It might appear that the star formation process is almost inevitable: most massive molecular clouds that are observed in large-scale CO surveys are associated with either radio or infrared sources indicative of recent or ongoing massive star formation (Myers et al. 1986). Similarly, lower mass clouds, such as Taurus (Kenyon et al. 1990) and Ophiuchus (Lada & Wilking 1984), are often the sites of low-mass star formation. Can one determine, a priori, how many stars are likely to form in a molecular cloud? For low-mass stars, one can compute the rate of star formation based on the rate of ambipolar diffusion or on the rate of energy input by newly formed stars (McKee 1989), but for high-mass stars, the situation is very different. O and B stars produce prodigious amounts of ionizing and dissociating radiation that can quickly destroy their immediate molecular environment and form large H II regions. Strong winds during the life of these stars and supernovae at the end of their life can play a major role in the cloud

dynamics and internal structure (see, e.g., Bally et al. 1987; Carpenter 1994; Williams, Blitz, & Stark 1995) although the effects of the winds and supernovae are ameliorated by the H II regions (McKee, Van Buren, & Lazareff 1984). OB stars may be responsible for both further star formation within the cloud (Elmegreen & Lada 1977) and also for a cloud's disruption and ultimate destruction (Tenorio-Tagle 1979; Whitworth 1979; Leisawitz 1990). Indeed, the photo-destructive effects of OB stars can limit the overall high-mass star-forming capacity of a cloud (Franco, Shore & Tenorio-Tagle 1994).

In view of the complexity of the interaction between massive stars and their natal molecular clouds, we shall not attempt to provide an a priori determination of the number of stars that are likely to form in a molecular cloud. Instead, we shall confine ourselves to the more limited task of empirically inferring the number of stars that have actually formed in Galactic molecular clouds. Elmegreen & Clemens (1985) have previously carried out related work in which they studied the formation of bound clusters in molecular

clouds. They focused on relatively small molecular clouds, whereas our attention is directed toward clouds large enough to generate OB associations.

In the companion paper to this work (McKee & Williams 1997, hereafter Paper I), we fitted the luminosity distribution of OB associations in the Galaxy. A number of steps were involved: a fit was made to a catalog of H II regions from a radio continuum survey (Smith, Biermann, & Mezger 1978) and was then extrapolated to lower luminosities. The integral of this distribution could only account for about 30% of the total ionizing flux in the Galaxy, implying that the distribution of *all* OB associations was different than that measured from the catalog. Based on observations of H II regions in external galaxies and in the solar neighborhood, we concluded that OB associations emit several times more ionizing photons than inferred from radio catalogs. The ionizing photons that escape from radio H II regions are absorbed in the envelopes of the H II regions (Anantharamaiah 1985). We demonstrated that this picture was consistent with observations of pulsar dispersion measures (Taylor & Cordes 1993) and with observations of ionized “worms” in the inner Galaxy (Heiles, Reach, & Koo 1996).

In the first half of this paper (§§ 2 and 3), we estimate the mass spectrum of molecular clouds in the Galaxy. There are strong parallels between our analysis here and the determination of the luminosity function in Paper I. We begin by fitting a truncated power law to three cloud catalogs (Dame et al. 1986; Solomon et al. 1987; Scoville et al. 1987), produced from two CO surveys of the first Galactic quadrant (Cohen, Dame, & Thaddeus 1986; Sanders et al. 1986). We determine a fit that is consistent with all three and then extrapolate to lower masses and the remainder of the inner Galaxy. The total cloud mass contained in this distribution amounts to only 40% of the total molecular mass of the Galaxy, which shows that the majority of molecular emission in the surveys was not cataloged into clouds. We create two models for the overall mass spectrum of all clouds and decide between the two using observations of the solar neighborhood.

In the second half of the paper (§§ 4, 5, and 6), we combine the luminosity distribution of OB associations with the mass distribution of molecular clouds to determine, with a minimal set of assumptions, a distribution of number of OB associations within a given cloud. We compare these predictions with the masses and luminosities of three cloud-association pairs. This result is then used to calculate the number of cloud-association pairs of given mass-luminosity in the Galaxy, the probability that a cloud does not form any massive stars, and the most likely brightest association in a cloud. The distribution of star formation efficiencies for individual associations within a cloud is calculated, as well as the average star formation efficiency for all the associations within a cloud. We then determine the filling factor of H II regions in giant molecular clouds (GMCs) and the rate at which the H II regions destroy the clouds. We conclude in § 7.

2. THE GALACTIC CO SURVEYS

The CO molecule has become the standard tracer of molecular clouds because of its high abundance and low dipole moment. There have been two large-scale CO(1–0) surveys made to date (Sanders et al. 1986; Cohen et al. 1986) which we use to identify the mass distribution of

molecular clouds in a similar way to the determination of the luminosity distribution of OB associations in Paper I.

The first step in deriving the mass distribution is to place the mass estimates of different authors on a common footing. All masses are adjusted to the same galactocentric distance, $R_0 = 8.5$ kpc. For masses determined from the virial theorem, we ensure that the same form of the virial theorem is used in all cases. For masses determined from CO luminosities, we include helium (assumed to give a total mass 1.36 times the molecular mass), and we adjust to a common value of the CO to H₂ conversion factor, $X = N_{\text{H}_2}/W_{\text{CO}}$.

Since the adjustment to a common value of X can be a source of confusion, we discuss it briefly here. Two separate steps are involved. The first step is to adjust all the data to a common temperature calibration for the telescopes used to observe the CO, so that a given observed value of the CO luminosity corresponds to the same CO mass. This adjustment has no effect on the inferred masses: if the temperature calibration is changed by some amount, then the X factor would change correspondingly so as to leave the masses unchanged (Bronfman et al. 1988). The Columbia CO data are often analyzed in terms of the calibration of Dame & Thaddeus (1985). However, in calibrating the telescope used for a CO survey from Chile, Bronfman et al. (1988) determined that this calibration was too low by a factor 1.22. The calibration of the Chile telescope appears to be the best available (Dame 1995), so we shall adopt it here. With this calibration, the value of X for the Bronfman et al. survey is $X = 2.3 \times 10^{20} \text{ cm}^{-2}/\text{K km s}^{-1}$. Dame et al. (1986, hereafter DECT) adopted $X = 2 \times 10^{20} \text{ cm}^{-2}/\text{K km s}^{-1}$ in their analysis; after adjusting this to the Chile telescope calibration, their value of X becomes $1.6 \times 10^{20} \text{ cm}^{-2}/\text{K km s}^{-1}$.

The second step in adjusting X is to bring the different data sets to a common H₂-to-CO calibration. This calibration is generally determined from gamma-ray observations and is somewhat uncertain. This step changes the inferred masses in direct proportion to the change in X . We adopt $X = 1.9 \times 10^{20} \text{ cm}^{-2}/\text{K km s}^{-1}$, determined from EGRET observations by Strong et al. (1997). For example, the masses in DECT increase by a factor (1.9/1.6) due to this change in X . However, the masses decrease when they are adjusted to a galactocentric radius of 8.5 kpc, and as a result the total correction factor for the masses in DECT is $(1.9/1.6) \times 0.85^2 = 0.86$. The correction factors for all the data sets used in this paper are summarized in Table 1.

We encounter three difficulties in unraveling the data to determine the mass spectrum. The first, incompleteness at the lower end of the spectrum, was also encountered in § 3 of Paper I. Fortunately, because the distribution of cloud

TABLE 1
CORRECTION FACTOR TO TABULATED MASSES

Reference	R_\odot	He ^a	X^b	α_{vir}	Correction
SYCSW	8.5	Yes	...	0.83	1.06 ^c
SRBY	10.0	Yes	...	1.1	1.19 ^c
DECT	10.0	Yes	1.6	...	0.86
Bronfman et al.	10.0	No	2.3	...	0.81
This work	8.5	Yes	1.9	1.1	1.00

^a Helium mass correction of 1.36.

^b $N(\text{H}_2)/W_{\text{CO}}$ [$10^{20} \text{ cm}^{-2}/(\text{K km s}^{-1})$], adjusted to Chile telescope scale.

^c Includes cloud size extrapolation.

masses is flatter than the distribution of association luminosities, most of the molecular mass in the Galaxy is in the most massive clouds so this problem is less worrisome.

The second problem is the well-known ambiguity in the determination of distances in the inner Galaxy: away from the tangent points, each radial velocity corresponds to two distances. Other distance indicators must be used to choose between the two (e.g., large z -deviation from the plane, abnormal size–line width ratio, H_2CO absorption against background H II regions, etc.), but nevertheless there remains confusion over distances and hence masses in a considerable number of cases.

The third and perhaps most irreconcilable problem occurs at the tangent points where, although the distance is well determined from the radial velocity, severe blending of emission from clouds along the line of sight is prevalent. For example, all clouds within 1 kpc of either side of the tangent point at $l = 45^\circ$ will share the same radial velocity to within 5 km s^{-1} —less than the FWHM of a typical GMC. At these points, it becomes extremely difficult to determine with any certainty the underlying distribution of molecular gas (Adler & Roberts 1992).

There exist, in all, three analyses of the two large-scale CO surveys, each of which tackles these problems in different ways. The Cohen et al. (1986) Columbia CO survey was undertaken on a “mini” 1.2 m telescope dedicated to the task. Its large beam size ($0^\circ.125$) is a distinct advantage for such large-scale mapping. The survey was fully sampled for $b < 0^\circ.5$ and sampled every other beamwidth for $0^\circ.5 < b < 1^\circ$. Spectra were Hanning smoothed to a resolution of 1.3 km s^{-1} , and rms noise temperatures were maintained below 0.45 K. This survey was analyzed by DECT, who concentrated on measuring only the masses of the largest clouds after subtracting the emission from a radially symmetric “background” of smaller clouds. They present a list of 33 of the most massive complexes, a number that is small enough to enable individual attention to such matters as the distance determination and amount of blending for each cloud but not large enough to make a statistically significant determination of the cloud distribution.

The Sanders et al. CO survey, on the other hand, was undertaken on the FCRAO 14 m telescope with its smaller $45''$ beam size. The survey limits are from $l = 8^\circ$ to 90° and $b = -1^\circ.05$ to $+1^\circ.05$. Full sampling over this range was impossible given reasonable time limitations, and the survey has a beam spacing of $3'$ for $18^\circ < l < 54^\circ$ and $6'$ elsewhere. Although undersampled, this map spacing ensures that all clouds larger than 20 pc, out to a distance of 10 kpc, will be observed in at least one position. The spectra were Gaussian smoothed in velocity to a resolution of 1.0 km s^{-1} , and typical rms noise temperatures are 0.4 K. There exist two similar analyses of this survey: Solomon et al. (1987, hereafter SRBY) and Scoville et al. (1987, hereafter SYCSW). Both attempted a complete dissection of the emission into individual clouds with masses from $\sim 10^4 M_\odot$ to $\sim 10^7 M_\odot$. However, there are two important differences in the analysis of the two groups.

In both cases, clouds are defined as being a collection of connected points in l - b - v space above a certain temperature threshold. Because the degree of blending varies considerably across the survey, being particularly high at the tangent points and the molecular ring, the choice of this threshold temperature presents a dilemma: a low threshold is required in regions of low blending so as to be able to

describe more completely the clouds, but a high threshold is better in the blended regions to distinguish between separate clouds. SRBY varied the threshold temperature across the survey (from 4 to 7 K) and were careful to avoid assigning merged regions to a large single cloud. SYCSW used a uniform threshold temperature set at 4 K across the whole survey and then subdivided clouds into “hot spots” at a higher threshold. This has the advantage of a uniform cloud definition but results in the cloud catalog being more affected by blending of emission at tangent points. The authors note that at least one cataloged object is a “runaway” blend of many smaller objects, and it would seem likely that there must be other clouds that are also affected.

The second difference is in the way cloud distances were determined. SYCSW assigned some clouds to the 3 kpc arm or the Cygnus arm based on their position in l - b - v space and some to the tangent point if the difference between near and far distances is less than 40%. For some of the remaining clouds, they solved for distances solely from the anomalous vertical distance from the plane. There remain many clouds with distance ambiguities in their catalog. SRBY, on the other hand, claim unambiguous distances for *all* clouds in their catalog. Clouds are assigned to the near or far side depending on which gives the best agreement with a model for the vertical scale height of emission and the size–line width relation, $\Delta V \propto R^{0.5}$.

A proper determination of the form of the mass function should be made only for those clouds whose distances, and hence masses, are well known: therefore, we restrict attention to those clouds in the SYCSW catalog that are either at the tangent point or in the 3 kpc or Cygnus arms. (A consequence of this restriction is that the three largest cataloged objects, which appear to be strongly blended, are excluded from the fit to the mass function.) This subset of the data can be used to determine the shape of the mass function, i.e., its slope and upper mass cutoff, but not its normalization. However, the SRBY catalog can be used, in principle, to quantify the mass function fully.

Both SRBY and SYCSW measure the size (R) and velocity dispersion (σ) of the clouds to determine virial masses $M_{\text{vir}} = 5R\sigma^2/\alpha_{\text{vir}}G$, where the virial parameter α_{vir} includes the effect of surface pressure, magnetic fields, and nonuniform densities (Bertoldi & McKee 1992). A value slightly greater than unity seems most appropriate for GMCs, and we have adopted $\alpha_{\text{vir}} = 1.1$ in agreement with SRBY. In addition, we have followed the suggestion of Solomon & Rivolo (1989) and have increased the masses of each cloud in both lists by an additional (constant) 40% to include cloud emission down to zero intensity (although it should be noted that the SRBY catalog used a variable cloud determination threshold). We summarize our corrections to the mass estimates from the referenced literature in Table 1.

The blending of CO emission, particularly at the tangent points, presents a severe obstacle to cloud definition and distance determination. We have compared the three cloud lists and find that the masses of clouds in the same location generally agree to within a factor ~ 2 – 3 , perhaps as good as might be expected given the different approaches. Nevertheless, measurements of the cloud mass function are undoubtedly affected by the blending in the surveys, and it is only determined with a large uncertainty. In the later sections of this paper, we will also appeal to cloud catalogs in less confused regions (e.g., the solar neighborhood and

outer Galaxy surveys; see § 3.4) for additional evidence on the shape of the distribution.

3. THE MASS SPECTRUM OF GIANT MOLECULAR CLOUDS

3.1. Fits to the First Quadrant Data

The surveyors (DECT, SRBY, SYCSW) fit the mass spectrum of GMCs to a power law, $d\mathcal{N}_c/dM \propto M^{-1.6}$. In this section we recalculate the mass spectrum, using all three cloud catalogs, considering an upper limit to the mass of GMCs, and imposing the condition that the final distribution integrates to a total Galactic molecular mass consistent with observations. The existence of an upper limit can be seen in the cloud numbers that peter out at several $10^6 M_\odot$ (Fig. 1).

The mass spectrum, therefore, cannot be characterized by an unrestricted power law, and an additional parameter describing the cutoff is necessary. As in § 3 of Paper I, we fit the data to a truncated power-law form,

$$\frac{d\mathcal{N}_c}{d \ln M} = \mathcal{N}_{cu} \left(\frac{M_u}{M} \right)^\alpha \quad M \leq M_u. \quad (1)$$

Here $d\mathcal{N}_c(M)$, the number of clouds with masses in the range $[M, M(1 + d \ln M)]$, follows a power law with slope $-\alpha$ up to a maximum mass M_u . As in Paper I, the constant, \mathcal{N}_{cu} is a measure of the number of clouds at the high-mass end. The integral form of this distribution is

$$\mathcal{N}_c(>M) = \frac{\mathcal{N}_{cu}}{\alpha} \left[\left(\frac{M_u}{M} \right)^\alpha - 1 \right]. \quad (2)$$

The differential is with respect to $\ln M$ so as to make equation (1) dimensionless. Written in this way, the differen-

tial form of the distribution shares the same exponent as the cumulative form and is numerically equal to 1 less than would be calculated for $d\mathcal{N}_c/dM$.

The observed differential cloud mass distributions for each of the three catalogs are plotted in Figure 1. The data are binned into mass bins of width $\log_{10} 2$, resulting in a set of pairs (M_i, N_i) where M_i is the central mass of bin i , and N_i is the number of clouds in that bin. The counting error in each bin is $(N_i)^{1/2}$, and error bars have been drawn at

$$\sigma_{i\pm} = \log(N_i \pm \sqrt{N_i}) - \log N_i = \log(1 \pm 1/\sqrt{N_i}). \quad (3)$$

These points have then been fitted to a truncated power law in the same manner as Paper I (§ 3). For each binning, a weighted least-squares fit to the triad (M_i, N_i, w_i) is made where the weights $w_i = 1/\sigma_{i\pm}^2$. Each fit results in values for M_u from the highest mass bin, α from the slope, \mathcal{N}_{cu} from the normalization, and χ^2 measuring the goodness of fit. By adjusting the high-mass end of the final bin (M_u), the appearance of the histogram changes, and therefore so do the fitted values of α , \mathcal{N}_{cu} , and χ^2 . The overall best fit is found by minimizing χ^2 . In this way, the three parameters of the truncated power-law distribution may be simultaneously found. The fits to the SYCSW and SRBY data are indicated on each histogram by a solid line over those bins used in the fit and a dotted line indicating extrapolated numbers at lower masses.

The small number of clouds and limited mass range in the DECT list makes a determination of α uncertain, so we do not directly fit their data. The high-mass end of the distribution has been carefully measured, however, and there are several clouds of mass $M = 4-5 \times 10^6 M_\odot$ indicating an upper mass cutoff M_u at least this big.

The mass coverage appears to be greater in the SRBY and SYCSW cloud lists, both made from the FCRAO survey using similar temperature threshold techniques. However, to fit the data, it is necessary to know at which point the catalogs are significantly incomplete. Only bins with masses greater than this limit are included in the analysis. The sensitivity and resolution of the survey, to some extent, and especially the high degree of cloud blending make detection of small clouds at large distances difficult. For the SRBY catalog, we estimate the completeness limit at $M = 3 \times 10^5 M_\odot$ based on the point at which the number of clouds at the near distance begins to significantly outnumber similar mass clouds at the far distance (Fig. 2). We cannot, unfortunately, apply the same process to the restricted SYCSW data set, which is not necessarily evenly distributed about the near/far side of the Galaxy. We adopt the same completeness limit as for the SRBY catalog, at which point there is a noticeable dip in SYCSW cloud numbers.

The fitted values for α , \mathcal{N}_{cu} , and M_u for each cloud list are summarized in Table 2. All three analyzes find a maximum cloud mass of order $M_u \simeq 5-6 \times 10^6 M_\odot$. Surveys of indi-

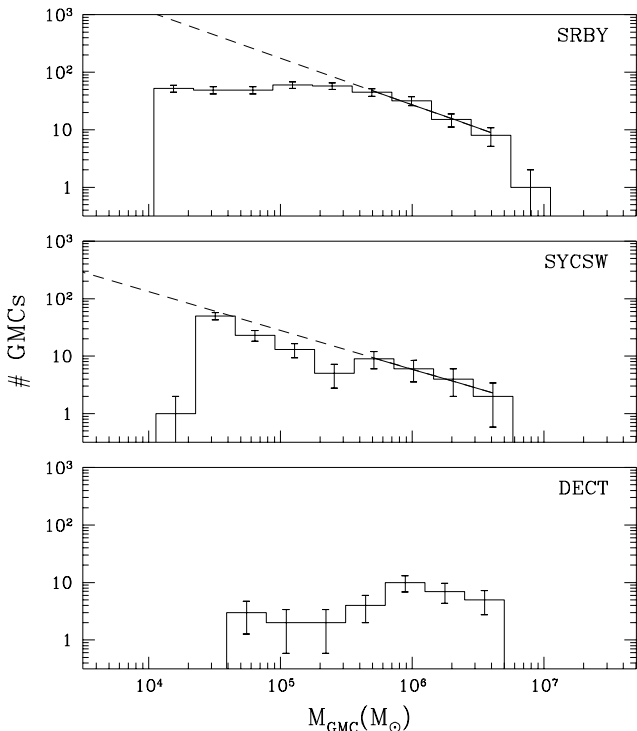


FIG. 1.—Cloud mass spectra for each of the three cloud catalogs. The masses in each catalog have been corrected by a constant factor as discussed in § 2. A least-squares fit to a truncated power law has been made to the SYCSW and SRBY catalogs over the range indicated by the solid line. The dotted line indicates the extrapolation of the fit to lower masses. The fitted parameters are in Table 2.

TABLE 2

FITS TO THE GMC MASS DISTRIBUTION^a

Survey	α	\mathcal{N}_{cu}	M_u
SYCSW	0.67 ± 0.25	> 2.7	$5.8 \times 10^6 M_\odot$
SRBY	0.81 ± 0.14	9.8 ± 3.1	$5.6 \times 10^6 M_\odot$
DECT	$> 5 \times 10^6 M_\odot$

^a First Galactic quadrant: $18^\circ \leq l \leq 54^\circ$.

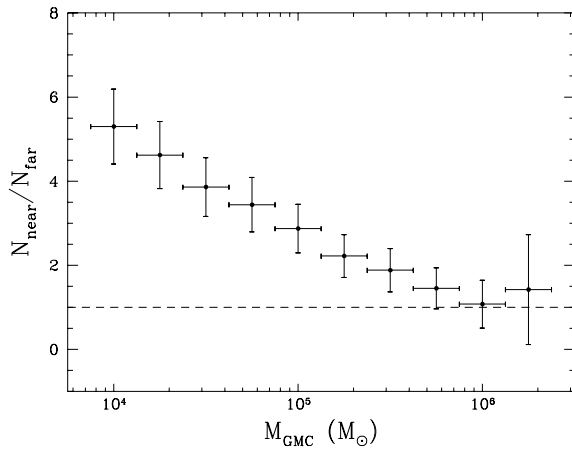


FIG. 2.—Ratio of the number of clouds in the SRBY catalog on the near side of the Galaxy ($d < R_0$) to the far side ($d > R_0$). Vertical error bars indicate counting uncertainties, and horizontal bars indicate the range of each mass bin. The completeness limit for which there are equal numbers of clouds cataloged on either side of Galaxy is $4 \times 10^5 M_\odot$.

vidual spiral arms will not be as confused by blending or distance ambiguities, and so they might be expected to measure cloud masses more accurately. The largest clouds found in the Carina spiral arm survey of Grabelsky et al. (1988) have masses $M \simeq 6 \times 10^6 M_\odot$, slightly greater than the most massive (unblended) clouds found by the three groups from the FCRAO and Columbia surveys. We adopt the maximum value, $M_u = 6 \times 10^6 M_\odot$.

The estimate $\mathcal{N}_{cu} = 10$ from the SRBY data is consistent with the lower limit found from the fit to the SYCSW clouds with unambiguous distances. This restricted list contained 12 clouds with masses $M > 5 \times 10^5 M_\odot$, compared to 45 in the original; thus, a crude correction for \mathcal{N}_{cu} for the entire catalog would be $2.7 \times (45/12) \simeq 10$. As in Paper I, we note that since $\mathcal{N}_{cu} \gg 1$, the upper end of the distribution is a real, physical limit: the mass of the largest Galactic molecular clouds is restricted to $M_u = 6 \times 10^6 M_\odot$ by some cloud formation or destruction process.

The power-law exponent, α , is less well determined principally because of the limited mass range available for the fits and is left as a free parameter for the time being. The fitted mass spectrum for the first quadrant is therefore

$$\frac{d\mathcal{N}_c}{d \ln M} = 10 \left(\frac{6 \times 10^6 M_\odot}{M} \right)^\alpha M \leq M_u = 6 \times 10^6 M_\odot, \quad (4)$$

which implies a total mass of clouds equal to

$$M_{\text{clouds}} = \int^{M=M_u} M d\mathcal{N}_c = \frac{\mathcal{N}_{cu} M_u}{1 - \alpha}, \quad (5)$$

where we have assumed $\alpha < 1$ so that the lower mass limit is unimportant. For values of α close to 1, the large numbers of low-mass clouds become increasingly important, and the extrapolation from the high-mass end of the distribution correspondingly becomes more uncertain. We consider the effect of this and its implications for the determination of a mass spectrum that is consistent with the total Galactic molecular mass, in the following section.

3.2. Extrapolation to the Galaxy

Essentially all the molecular gas in the Galaxy is contained within clouds, and therefore the mass spectrum must

be able to account for the total Galactic molecular mass. In this section we show that the cloud distributions derived from the cloud catalogs are inconsistent with this criterion and postulate two alternative possibilities. We were faced with a similar problem in § 4.1 of Paper I when confronting the discrepancy between the overall Galactic ionizing flux and the total from the catalog of H II regions. In many ways, our discussion here mirrors the discussion there.

Bronfman et al. (1988) totalled the CO emission from the Columbia surveys of the northern and southern skies and deduced a total molecular mass, M_{tot} , equal to $1.2 \times 10^9 M_\odot$ in the inner Galaxy (1.7–8.5 kpc). After adjusting this mass for uniformity with the Galactic surveys as indicated in Table 1, we adopt $M_{\text{tot}} = 1.0 \times 10^9 M_\odot$.

The first quadrant surveys covered about 40% of the plane and therefore must be scaled by a factor of 2.5 to account for the entire Galaxy. The slope, α , and upper mass limit, M_u , are unchanged, but the normalization is scaled up to $\mathcal{N}_{cu} = 25$. For $\alpha = 0.6$ (corresponding to $d\mathcal{N}_c/dM \propto M^{-1.6}$, the canonical value most often quoted), the extrapolated mass spectrum integrates to a total mass, $M_{\text{clouds}} = 4 \times 10^8 M_\odot$, which is less than M_{tot} by a factor of 2.5. This inconsistency between the sum of cloud masses from the catalogs and the total molecular emission is well known: DECT subtracted a background from the Columbia survey that amounted to 63% of the total emission, and further analysis of the SRBY catalog by Solomon & Rivolo (1989) showed that, by mass, 60% of the clouds in the Galaxy lie below their (variable) 4–7 K detection threshold.

There are, therefore, large numbers of molecular clouds that were not cataloged. Since we have no information on the mass distribution of these clouds, we take the simplest possible approach and assume that, as with the cataloged clouds, the overall cloud mass spectrum may also be characterized as a truncated power law. Our insistence that the integral of the mass spectrum equal the total mass of molecular gas in the Galaxy then implies that, for this overall mass distribution, the combination $\mathcal{N}_{cu} M_u / (1 - \alpha)$ be 2.5 times greater than the parameters derived from the extrapolated fits to the cloud catalogs. We are reluctant to consider an increase in M_u since it would seem unlikely that the most massive clouds in the Galaxy would not be cataloged. This leaves the possibility that either \mathcal{N}_{cu} is greater than 25 and/or that α is greater than 0.6 for the overall cloud distribution. We consider two extremes:

Model A: Scaled Distribution.—In this model, an equal proportion of clouds of all masses are uncataloged, and the overall mass distribution is simply a linear scaling of the mass distribution in equation (4). That is, α is set equal to 0.6, and \mathcal{N}_{cu} increased by a factor of 2.5 to 63.

Model B: Steeper Distribution.—In this model, the opposite of A, there are predominantly more uncataloged clouds at lower masses, and the overall mass distribution is steeper than that measured for the cataloged clouds alone. Putting all the difference into the slope and not the normalization we set $\mathcal{N}_{cu} = 25$, $\alpha = 0.85$ which satisfies $\mathcal{N}_{cu} M_u / (1 - \alpha) = M_{\text{tot}}$.

Cloud surveys in the outer Galaxy, though not as extensive as those in the inner Galaxy, do not suffer from crowding at the terminal velocity or from the near-far distance ambiguity. Therefore, cloud catalogs of the outer Galaxy might be expected to suffer less from confusion and to help constrain the value of α . There are uncertainties, however, in the CO/H₂ ratio and, consequently, in the mass estimates of

TABLE 3
MASS SPECTRUM PARAMETERS

Analysis	α	\mathcal{N}_{cu}^a	$M_u (M_\odot)$	Comments
Fit to catalogs	0.6	10	6×10^6	First quadrant only
Extrapolation	0.6	25	6×10^6	Entire Galactic disk
Model A	0.6	63	6×10^6	Integrates to M_{tot}
Model B	0.85	25	6×10^6	Integrates to M_{tot}

^a $1.7 \text{ kpc} \leq R \leq 8.5 \text{ kpc}$.

the clouds (Digel, Bally, & Thaddeus 1990). It is also unclear to what extent results on the mass distribution of clouds in the outer Galaxy are applicable to the distribution of clouds in the inner Galaxy. A recent analysis of the mass distribution of outer Galaxy clouds by Brand & Wouterloot (1995) finds a slope $\alpha \simeq 0.6$, in close agreement with Model A. Interestingly, however, their fit to clouds in the inner and outer Galaxy together is much steeper, $\alpha = 0.8$, and more appropriate to Model B. There are a number of other indications for such a steep slope: it is measured in our analysis of the SRBY data (although they themselves find a slope, $\alpha = 0.6$), and it also matches the slope of the mass spectrum inferred for atomic clouds by Dickey & Garwood (1989). Finally, simulations of dense clumps within a molecular cloud (a similar situation to that of clouds in the Galaxy but without the strong ordered rotation) showed that blending of clump emission tends to flatten the observed mass spectrum to a shallower slope than the true value (Williams, de Geus, & Blitz 1994). As we have noted, blending of cloud emission in the Galaxy is very severe, so it is quite possible that the slope of the true distribution could indeed be steeper than $\alpha = 0.6$.

The fitted parameters, and the subsequent adjustments made to them to account for first, the limited coverage of the surveys and second, the difference between the integrated mass of the cataloged clouds and the total molecular mass in the Galaxy, are summarized in Table 3. Although the difference in the value of α between models A and B appears small, it has a large effect on the predicted numbers of clouds and particularly on the predicted fraction of uncataloged clouds. Cloud numbers and the contribution from the uncataloged component are displayed for a variety of mass ranges and for each model in Table 4. Model A implies that the majority of molecular clouds were not detected in the surveys in equal proportions at all masses, so that even for the most massive clouds, $M \simeq M_u$, there are an additional three clouds for every two clouds in the catalogs. In Model B, however, most of the massive clouds are presumed to be in the catalogs, and the majority of clouds that are missing are of low mass. Measuring the numbers of low-mass clouds, then, should be a good test of how closely the true distribution follows either of the two models. Since

TABLE 4
CLOUD NUMBERS FOR MODELS A AND B

$M (M_\odot)$	MODEL A		MODEL B	
	$\mathcal{N}_c(>M)$	Percent ^a	$\mathcal{N}_c(>M)$	Percent ^a
10^3	2×10^4	60	5×10^4	84
10^4	5×10^3	60	7×10^3	72
10^5	1200	60	900	48
10^6	200	60	100	24

^a Percentage of clouds that are undetected.

low-mass clouds are expected to be more readily observable at closer range, this can be done most easily by studying the clouds in the solar neighborhood. First, however, we must relate our global cloud distribution to the local surface density of clouds.

3.3. Surface Density of Molecular Clouds

Figure 3 shows the radial distribution of molecular gas surface density, Σ , as measured by Bronfman et al. (1988) and Wouterloot et al. (1990). Note that the surface densities have been corrected to include He and to agree with the value of X we have adopted; the values are independent of R_0 , however. Although the data extend in to $0.2R_0 = 1.7 \text{ kpc}$, the exponential behavior sets in only for $R \gtrsim 3.5 \text{ kpc}$. We have fitted the variation of $\Sigma(R)$ to an exponential for $3.5 < R < 18 \text{ kpc}$ and find a radial scale length $H_R = 3.5 \pm 1.0 \text{ kpc}$. This value is consistent with that measured for the radial variation of OB associations in § 6 of Paper I, which in turn is consistent with the estimates compiled by Lacey & Fall (1985) for the radial scale length for supernova remnants, pulsars, and thermal radio emission. It also agrees with the radial scale length of the stellar disk of the Galaxy in the standard model of Bahcall & Soneira (1980). The sharp falloff in the molecular surface density beyond $R \simeq 18 \text{ kpc}$ corresponds to the edge of the optical disk of the Galaxy (see Digel, de Geus, & Thaddeus 1994 and references therein).

Although the surface density drops exponentially with radius, the large area of the disk beyond the solar circle implies that the total molecular mass in the outer Galaxy is substantial. Wouterloot et al. (1990) and Dame (1993) estimate that the integrated molecular mass for $R > R_0$ is $\simeq 6 - 8 \times 10^8 M_\odot$. This is almost the same as the molecular mass within the solar circle and may even be greater if the conversion factor from CO to H_2 increases significantly with radius (Digel et al. 1990; Sodroski et al. 1995).

The radial dependence of the surface density of molecular gas between 1.7 and 3.5 kpc does not fit the exponential distribution. Nonetheless, in order to have a simple model for the radial distribution of molecular gas that is consistent with our model for OB associations (see § 6 of Paper I), we assume that all the molecular gas at $R > 1.7 \text{ kpc}$ is distributed in an exponential disk that extends from R_{min} to R_{max} .

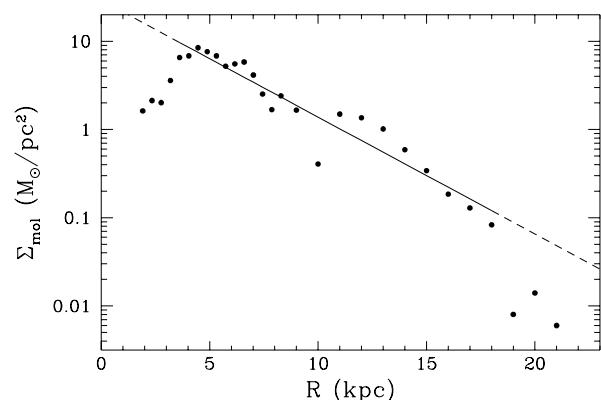


FIG. 3.—Radial variation of surface density of molecular gas in the Galaxy. Data are from Bronfman et al. (1988) and Wouterloot et al. (1990) and have been scaled for a uniform R_0 and X factor (see Table 1). A least-squares fit to the exponential scale length, H_R , has been made to the data for $3.5 \text{ kpc} < R < 18 \text{ kpc}$.

We adopt $R_{\min} = 3$ kpc to be consistent with Paper I. Under the assumption that the cloud mass distribution is independent of radius, the surface density of clouds is then

$$\frac{d\mathcal{N}_c(>M)}{dA} = \mathcal{N}_c(>M) \left[\frac{\exp(-R/H_R)}{A_{\text{eff}}} \right], \quad (6)$$

where A_{eff} is an effective disk area,

$$\begin{aligned} A_{\text{eff}} &= \int_{R_{\min}}^{R_{\max}} \exp\left(\frac{-R}{H_R}\right) 2\pi R dR \\ &= 2\pi H_R^2 \left[\left(1 + \frac{R}{H_R}\right) \exp\left(\frac{-R}{H_R}\right) \right]_{R_{\min}}^{R_{\max}}. \end{aligned} \quad (7)$$

The most accurately determined molecular masses are inside the solar circle. With $R_{\max} = 8.5$ kpc and with $H_R = 3.5$ kpc from above, we find an effective area for the disk of the inner Galaxy $A_{\text{eff}} = 37$ kpc². This is smaller than the value $A_{\text{eff}} = 47$ kpc² adopted in Paper I, but there we set $R_{\max} = 11$ kpc so as to include all the giant H II regions. With $A_{\text{eff}} = 37$ kpc², the predicted surface density at the solar circle is $M_{\text{tot}} \exp(-R_0/H_R)/A_{\text{eff}} = 2.4 M_{\odot} \text{ pc}^{-2}$. By comparison, Bronfman et al. (1988) found an H₂ surface density of $2.15 M_{\odot} \text{ pc}^{-2}$ at 9.75 kpc, which is just inside the solar circle with their distance scale. Including helium and correcting to our adopted value for X , we find that their value for the molecular surface density at the solar circle becomes $2.4 M_{\odot} \text{ pc}^{-2}$, in agreement with our estimate.

The similarity of the exponential scale length of molecular gas with that of OB associations measured in Paper I, and with the scale length of massive stellar remnants discussed by Lacey & Fall (1985), suggests that there is no strong radial dependence of the star formation efficiency of massive stars in molecular clouds. The similar scale length of the stellar disk in the standard model of Bahcall & Soneira (1980) points to the same conclusion for the formation efficiency of all stars. Furthermore, although the molecular mass continues out to large radii, there is no evidence for very massive GMCs, $M > 10^6 M_{\odot}$, in the outer Galaxy (Digel et al. 1990), which is consistent with the lack of giant H II regions beyond 11 kpc (Smith et al. 1978).

3.4. Cloud Distribution in the Solar Neighborhood

We have found that the existing Galactic surveys on their own cannot convincingly determine the slope of the mass spectrum of molecular clouds. We can, however, extend observations of the cloud distribution by almost an extra order of magnitude lower in mass by employing observations of the solar neighborhood. Dame et al. (1987) use northern and southern surveys made with almost identical telescopes to map completely the molecular cloud distribution within 1 kpc of the Sun. We have adjusted cloud masses to allow for inclusion of helium and a value for $X = 1.9 \times 10^{20} \text{ cm}^{-2}/\text{K km s}^{-1}$, where the CO temperature scale in X has been adjusted to the Chile telescope scale. Within 1 kpc of the Sun, individual cloud distances are determined by methods other than Galactic rotation, and there is, therefore, no distance correction to cloud masses for $R_0 = 8.5$ kpc.

The cloud distribution in the solar neighborhood (within a radius of 1 kpc) is the galactic distribution scaled by $\pi \exp(-R_0/H_R)/A_{\text{eff}} = 134$. We have scaled the predicted mass spectrum for Model A and Model B and compared with the cloud numbers observed by Dame et al. (1987) in Figure 4. The flatter slope of Model A is found to fit the data marginally better than Model B, although Model B cannot be rejected on statistical grounds. In view of this, and in agreement with previous work (DECT; SRBY; SYCSW), we adopt Model A as a better representation of the mass distribution of GMCs in the inner Galaxy, so that

$$\begin{aligned} \frac{d\mathcal{N}_c}{d \ln M} &= 63 \left(\frac{6 \times 10^6 M_{\odot}}{M} \right)^{0.6}, \\ &(M \leq 6 \times 10^6 M_{\odot}, 1.7 \text{ kpc} \leq R \leq 8.5 \text{ kpc}). \end{aligned} \quad (8)$$

A major implication of our choice of the flatter distribution of the two models is that the molecular gas in the Galaxy is strongly concentrated in the most massive clouds; 50% of the total mass is contained in the 200 clouds with masses greater than $10^6 M_{\odot}$. This distribution has been derived from two Galactic CO surveys and the resulting three catalogs. It accounts for the total molecular mass of the Galaxy measured by Bronfman et al. (1988) and is consistent with

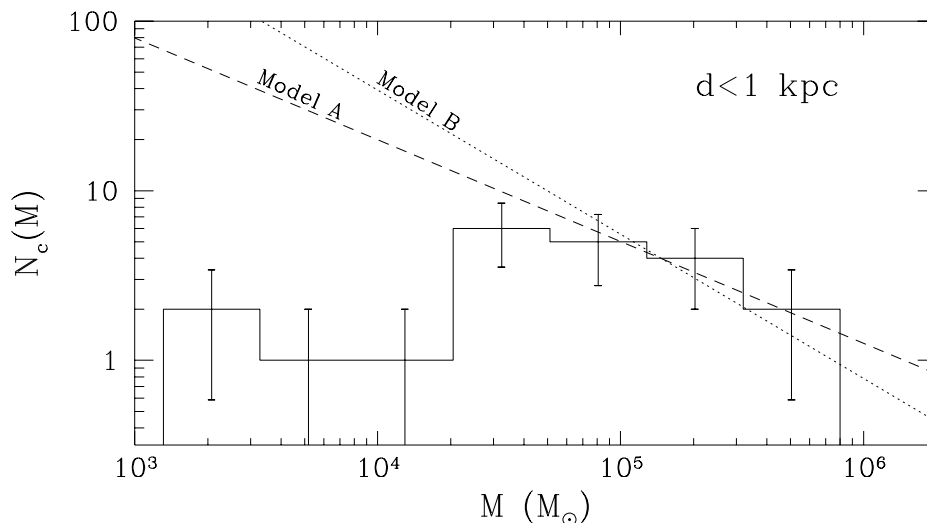


FIG. 4.—Distribution of the number of clouds as a function of cloud mass for the solar neighborhood ($d < 1$ kpc). Data are from Dame et al. (1986). The dotted and dashed lines indicate the expected numbers for each of the cloud distribution models A and B.

the number of low-mass clouds in the solar neighborhood observed by Dame et al. (1987).

4. THE JOINT DISTRIBUTION OF OB ASSOCIATIONS AND GMCs

We have now derived a plausible mass spectrum of GMCs in the Galaxy. In Paper I, we derived a similarly plausible luminosity distribution of Galactic OB associations, $\mathcal{N}_a(>S)$, where \mathcal{N}_a is the number of associations and S is the ionizing luminosity ($\lambda < 912 \text{ \AA}$) of the stars in the association. The latter was found to fit a truncated power law at high luminosities,

$$\frac{d\mathcal{N}_a}{d\ln S} = \mathcal{N}_{au} \left(\frac{S_u}{S} \right) = 6.1 \left(\frac{490}{S_{49}} \right), \quad (9)$$

$$10 \lesssim S_{49} \leq 490, R \leq 11 \text{ kpc},$$

where S_{49} is the ionizing luminosity of an association in units of 10^{49} photons s^{-1} . The distribution then flattens off at lower luminosities owing to the rapidly decreasing ionizing flux from lower mass stars.

In this section, we combine the mass spectrum and the luminosity function to calculate the expected distribution of OB associations within GMCs. We argue as follows: if $\mathcal{N}_{a,M}$ is the number of associations within some luminosity range in a given cloud of mass M , then the sum of $\mathcal{N}_{a,M}$ over all clouds should give the total number of associations in the Galaxy in this luminosity range. That is, we can recover the luminosity function by integrating over the cloud distribution. This is a fundamental constraint. In addition, we make two assumptions about the behavior of $\mathcal{N}_{a,M}$. We assume that small clouds cannot form large associations; that is, there is a limit to the star-forming efficiency of a cloud. Second, we assume that the star formation rate in a cloud is linearly proportional to its mass (Mooney & Solomon 1988; Scoville & Good 1989; Carpenter, Snell, & Schloerb 1990); i.e., $\mathcal{N}_{a,2M} = 2\mathcal{N}_{a,M}$, with the proviso that the upper end of the luminosity range is still within the allowed star formation efficiency of that cloud. These two assumptions and the integral constraint completely define the joint distribution. There are undoubtedly other considerations that help determine the distribution of massive stars within GMCs; we have simply chosen this minimal set of assumptions as a first attempt on the problem.

We determine four quantities as a function of a cloud's mass: the number of associations expected in the cloud, the total number of cloud-association pairs for each association luminosity, the probability that the cloud does not contain any O stars, and the luminosity of the brightest association expected in the cloud. The combination of two global distributions to a local (or individual) distribution is inherently statistical, and the deviation from these mean estimates may be very large for any particular cloud depending on its individual circumstance (e.g., the effect of nearby stars/supernovae on a cloud, location in or out of spiral arm, etc.) The results presented here, then, should be considered a guide and are intended to complement studies of the correlation of cloud-association pairings on a cloud-by-cloud basis (see, e.g., Myers et al. 1986).

Before presenting the results of our study of the correlations between clouds and associations, we must first adjust the luminosity function of OB associations so that it refers only to the inner Galaxy, just as the cloud mass spec-

trum does. Recall that our estimate of the cloud spectrum is based on observations of molecular clouds within $R_0 = 8.5$ kpc, whereas the giant H II regions in the catalog of Smith et al. (1978) extend out to $1.3R_0 = 11$ kpc. Of these, 75% are within R_0 . Equivalently, the effective area for the clouds, which we modeled as extending over the range 3–8.5 kpc, is $A_{\text{eff}} = 37 \text{ kpc}^2$, whereas the effective area for the OB associations that power the giant H II regions is $A_{\text{eff}} = 47 \text{ kpc}^2$; the effective area for the clouds is thus 79% of that for the associations. We shall adopt the first value for the scale factor, since the second depends on the uncertain value of $R_{\text{min}} = 3$ kpc. The scaled value for \mathcal{N}_{au} thus becomes $0.75 \times 6.1 = 4.6$.

For the remainder of this and the following section, we consider only Model A for the GMC mass spectrum. A steeper distribution, more appropriate to Model B, will result in a steeper joint distribution for the number of associations in a given cloud and will increase the numbers for the Orion and the Rosette objects by a factor $\simeq 2$. The conclusions regarding cloud photoevaporation lifetimes are affected to a smaller degree.

4.1. The Number of Associations per Cloud

We define $d\mathcal{N}_{a,M}(S)$ to be the expected number of associations in the luminosity range dS in a cloud of mass M . We begin by expressing the integral constraint and two assumptions in mathematical form. The star formation efficiency (SFE) of a cloud of mass M with a mass M_* in stars is

$$\epsilon = \frac{M_*}{M_* + M} \simeq \frac{M_*}{M} = 570 \left(\frac{S_{49}}{M/M_\odot} \right), \quad (10)$$

where the last equality follows from the relation $M_* = 570S_{49} M_\odot$ (§5; Paper I). Recall from the discussion in Paper I that associations undergo several generations of star formation; the mass of stars in equation (10) refers to just the current generation. The upper limits to the distribution of cloud masses, M_u , and to the distribution of association luminosities, S_u , define an efficiency

$$\epsilon_u = 570 \left(\frac{S_{u,49}}{M_u/M_\odot} \right) = 0.047. \quad (11)$$

This is less than the maximum possible SFE for a cloud, ϵ_{max} , since there is only a small probability that the largest cloud will in fact have produced an association at the maximum efficiency (see § 5). For numerical estimates, we adopt $\epsilon_{\text{max}} = 0.1$; as we shall see, this appears to be consistent with observation, and it agrees with the analytic estimate of Elmegreen & Clemens (1985). Defining b as the ratio of ϵ_{max} to ϵ_u , we then have

$$b \equiv \frac{\epsilon_{\text{max}}}{\epsilon_u} = 2.1. \quad (12)$$

The most luminous association possible in a cloud has an ionizing luminosity that is the smaller of the observed upper limit, S_u , and the value corresponding to ϵ_{max} . Since we have $S = (S_u/\epsilon_u M_u)\epsilon M$, the maximum ionizing luminosity is

$$S_{\text{max}}(M) = \min [S_u, b(M/M_u)S_u]. \quad (13)$$

Thus, our first assumption implies $\mathcal{N}_{a,M} = 0$ for $S > S_{\text{max}}(M)$.

The second assumption, that of linearity of star formation rate with cloud mass, may be stated as $d\mathcal{N}_{a,M}(S) \propto M$

for $S \leq S_{\max}(M)$. Except for the restriction $S \leq S_{\max}(M)$, this is equivalent to assuming that all molecular gas has equal propensity for forming stars (the star formation rate per unit mass of gas is constant). There are undoubtedly many other factors that might affect the star formation efficiency of a cloud. These two assumptions are a minimum set necessary to proceed, but for a detailed comparison with observations, other factors (e.g., cloud environment) should be considered.

With only these two assumptions, however, we find that

$$\frac{d\mathcal{N}_{a,M}}{d\ln S} = \xi(S)MH[S_{\max}(M) - S], \quad (14)$$

where $H(x) = 0$ for $x < 0$ and 1 for $x > 0$ is the step function. The unknown function $\xi(S)$, which depends only on S , is determined by the condition that the integral over the cloud distribution gives the original luminosity distribution

$$\int \frac{d\mathcal{N}_{a,M}(S)}{d\ln S} d\mathcal{N}_c(M) = \frac{d\mathcal{N}_a(S)}{d\ln S}, \quad (15)$$

where $d\mathcal{N}_a(S)/d\ln S$ is the luminosity function of OB associations. Solving for $\xi(S)$, we find

$$\frac{d\mathcal{N}_{a,M}(S)}{d\ln S} = \frac{M}{M_{\text{tot}}} \times \frac{H[S_{\max}(M) - S]}{1 - (S/bS_u)^{1-\alpha}} \times \frac{d\mathcal{N}_a(S)}{d\ln S}. \quad (16)$$

Intuitively, this equation states that the number of associations with luminosities in the range dS in a cloud of mass M is the total number of such associations, $d\mathcal{N}_a(S)$, times a mass fraction. This mass fraction is the ratio of the cloud mass to all the molecular mass in clouds large enough to contain an association of luminosity S , i.e., clouds with mass $M > M_{\min}(S) = (S/bS_u)M_u$. The integrated mass in these clouds is $M_{\text{tot}}[1 - (M_{\min}/M_u)^{1-\alpha}]$, which is equivalent to the expression in the denominator of equation (16).

The expected number of associations with luminosities in a range $\Delta\ln S$ centered on S , in a cloud of mass M , is $\Delta\mathcal{N}_{a,M}(S) = d\mathcal{N}_{a,M}/d\ln S \times \Delta\ln S$. We plot, in Figure 5, contours of $d\mathcal{N}_{a,M}/d\ln S \times \ln 4$, corresponding to a luminosity range $[S/2, 2S]$. The kink in the figure at $S_{49} \simeq 10$ is a result of the sharp feature in the luminosity function which, in turn, is due to an assumed rigid upper bound to the stellar IMF. The line $S = S_{\max}(M)$ marks the boundary between the contours and the forbidden triangular region for which the SFE would be greater than ϵ_{\max} .

The positions of a few well-known cloud-association pairs, Orion, the Rosette, and the W49A complex, have been plotted in Figure 5. Cloud masses and association luminosities are tabulated in Table 5. The luminosity of the Orion Nebula, $S_{49} = 2.7$, has been determined from the table of stellar types in Cardelli & Clayton (1988) and the corresponding luminosities calculated by Vacca, Garmany, & Shull (1996). The mass of the Orion A cloud is taken to be $M = 1 \times 10^5 M_{\odot}$ (Maddalena et al. 1986). The luminosity

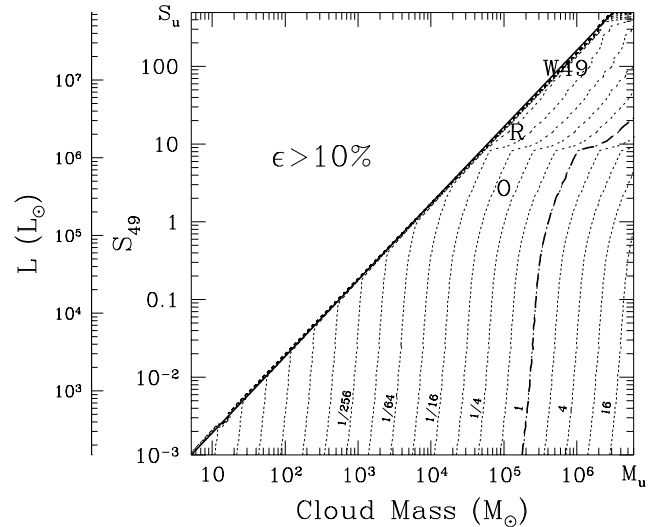


FIG. 5.—Expected number of associations of luminosity L , in a cloud of mass M . In the notation of § 4, this is $d\mathcal{N}_{a,M}/d\ln S \cdot \Delta\ln S$ where the interval in luminosity $\Delta\ln S = \ln 4$ (corresponding to $[S/2, 2S]$). The contours are labeled, and the positions of various cloud-association pairs are indicated. The limit to the star formation efficiency, $\epsilon \leq \epsilon_{\max} = 10\%$, appears as a diagonal line across the figure, which results in a forbidden zone in the top left-hand corner of the figure.

of the Rosette Nebula was calculated by Cox, Deharveng, & Leene (1991) to be $S_{49} = 14.4$, and the mass of the Rosette molecular cloud is taken to be $1.5 \times 10^5 M_{\odot}$ (Blitz & Thaddeus 1980). The ionizing luminosity of W49A was calculated from the measurement of the far-infrared luminosity, $L = 2.7 \times 10^7 L_{\odot}$, by Ward-Thompson & Robson (1990), corrected for a more recently determined distance, 11.4 kpc (Gwinn, Moran, & Reid 1992), and converted to $S_{49} = 120$ using Table 1 of Paper I. The mass of the host cloud, $M = 7 \times 10^5 M_{\odot}$, was taken directly from the SRBY survey and implies a star formation efficiency, $\epsilon_{W49A} = 9\%$, close to ϵ_{\max} .

Only about one in about eight clouds of the same mass of the Orion A cloud would contain an association of comparable luminosity to the Orion Nebula. The Rosette cloud-association combination is even rarer, $\mathcal{N}_{a,M}(\text{Rosette}) \simeq 1/16$. Why are these numbers so low? There are about 2×10^4 clouds more massive than $10^3 M_{\odot}$ from Table 4. This is roughly equal to the total number of OB associations, $\mathcal{N}_{a,\text{tot}} = \mathcal{N}_{au} S_u/S_l$, calculated over the same radial range. However, the slope of the cloud mass distribution is flatter than that of the association luminosity function, and most of the molecular mass resides in a relatively small number of massive clouds. Our assumption of a uniform star formation rate per cloud mass implies, therefore, that the massive clouds contain the majority of associations and results in the likelihood of a moderately luminous associ-

TABLE 5
CLOUD-ASSOCIATION PAIRS

Cloud	$M_c (M_{\odot})$	S_{49}	References
Orion A	$1 \times 10^5 M_{\odot}$	2.7	Maddalena et al. 1986; Cardelli & Clayton 1988
Rosette	$1.5 \times 10^5 M_{\odot}$	14.4	Blitz & Thaddeus 1980; Cox et al. 1991
W49A	$7 \times 10^5 M_{\odot}$	120.0	SRBY; Ward-Thompson & Robson 1990
G216-2.5	$3.4 \times 10^5 M_{\odot}$	<0.25	Maddalena & Thaddeus 1985

ations in a moderately massive cloud being rather small. Most clouds forms stars with an efficiency, $\epsilon \ll \epsilon_{\max}$.

4.2. The Number of Cloud-Association Pairs

We can convert the numbers for associations in any one cloud to total numbers of association-cloud pairs in the Galaxy by integrating over the cloud mass spectrum. In this way we find, for example, how many clouds of similar mass to the Orion A molecular cloud contain an association of similar luminosity to the Orion nebula.

For a range $\Delta \ln S$ in association luminosity, and $\Delta \ln M$ in cloud mass, there are $\Delta \mathcal{N}_{a,M}(S)$ associations within this luminosity range per cloud and $\Delta \mathcal{N}_c(M) = d\mathcal{N}_c(M)/d \ln M \times \Delta \ln M$ clouds in this mass range. Therefore the total number of associations of luminosity S within all clouds of mass M is $\Delta \mathcal{N}_a(S, M) = \Delta \mathcal{N}_{a,M}(S) \Delta \mathcal{N}_c(M)$, and by dividing through by $\Delta \ln S \Delta \ln M$, we deduce the differential expression,

$$\frac{d^2 \mathcal{N}_a(S, M)}{d \ln S d \ln M} = \frac{d \mathcal{N}_{a,M}(S)}{d \ln S} \times \frac{d \mathcal{N}_c(M)}{d \ln M}. \quad (17)$$

Figure 6 plots contours of $\Delta \mathcal{N}_a(S, M)$ for luminosity and mass ranges $\Delta \ln S = \Delta \ln M = \ln 4$, equivalent to a factor of 2 in each quantity. The correspondence of $\mathcal{N}_a(S, M)$ with association-cloud pairs breaks down in the high-mass/low-luminosity corner [since $\Delta \mathcal{N}_{a,M}(S) \gtrsim 1$] but is valid elsewhere in the figure.

Figure 6 shows that there are expected to be a total of ≈ 200 Orion-like objects in the Galaxy (i.e., associations with a luminosity equal, to within a factor of 2, to the luminosity of the Orion Nebula, in a cloud with a mass equal, to within a factor of 2, to the mass of Orion A), and ≈ 50 Rosette association-cloud pairs. Using the exponential surface density distribution described in § 3.3 with $A_{\text{eff}} = 47 \text{ kpc}^2$, these numbers can be scaled to an area, A , in the solar vicinity by multiplying by $A \exp(-R_0/H_R)/A_{\text{eff}}$. One would expect, therefore, one Orion within 900 pc and one Rosette within 1800 pc from the Sun, which is in approximate agreement with the numbers of star-forming clouds in the solar neighborhood (Dame et al. 1986).

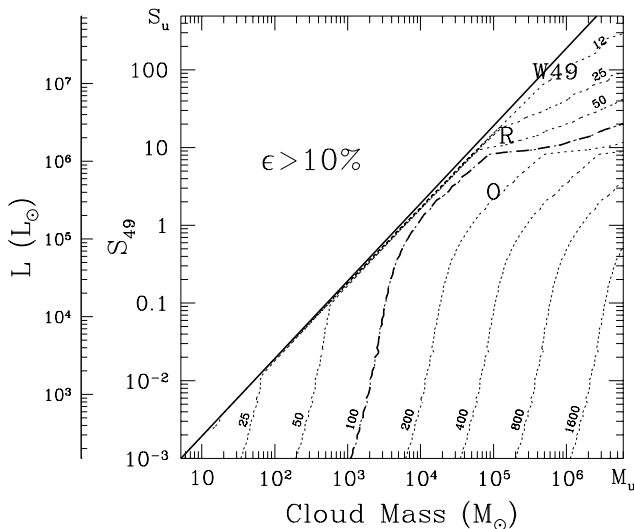


FIG. 6.—Expected number of cloud-association pairs in the Galaxy, $\mathcal{N}_a(S, M)$, such that a cloud with mass in the range $[M/2, M]$ contains an association with luminosity in the range $[S/2, 2S]$. Axes are as in Fig. 5. The positions of the Orion, Rosette, and W49A complexes are shown for reference.

4.3. The Probability of a Non-Star-forming Cloud

One might continue this line of inquiry to ask how likely is it that a given molecular cloud does not harbor any OB associations? (e.g., G216-2.5; Maddalena & Thaddeus 1985). We first integrate equation (16) to calculate the total number of OB associations of all (allowed) luminosities expected in a cloud of mass M ,

$$\mu(M) \equiv \mathcal{N}_{a,M}(S_l) = \int_{S_l}^{S_{\max}(M)} \frac{d \mathcal{N}_{a,M}}{d \ln S} d \ln S. \quad (18)$$

If we assume that, within a particular cloud, the distribution of the number of associations follows a Poisson distribution with mean μ , then the probability of such a cloud containing n associations (of any luminosity) is $P_n(M) = \mu^n e^{-\mu}/n!$, and, in particular, the probability that the cloud is devoid of any O stars is (Fig. 7)

$$P_0(M) = e^{-\mu} = e^{-\mathcal{N}_{a,M}(S_l)}. \quad (19)$$

P_0 is approximately 1 at low masses and rapidly decreases to 0 at high masses. Low-mass clouds are unlikely to contain any O stars, but a high-mass cloud is overwhelmingly likely to contain at least one O9.5 star. The transition between the two extremes is reasonably sharp: P_0 decreases from 0.8 to 0.2 in less than a decade in cloud mass. The median $P_0 = 0.5$ occurs at a mass $M_{1/2} \approx 10^5 M_\odot$. The majority, about 80%, of clouds as massive as G216-2.5 (see Table 5) are expected to contain at least one OB star. However, based on these statistical arguments at least, massive clouds without massive stars are by no means completely unexpected.

The above is readily generalized to different threshold luminosities. For example, the probability that a particular cloud contains an association at least as luminous as Orion is found by simply replacing S_l with S_{Orion} in equation (19). The three curves in Figure 7 correspond to thresholds of a single O9.5 star, Orion, and the Rosette nebula. Given the simple approach that we have taken here, we predict that the majority of clouds with masses $M \gtrsim 10^5 M_\odot$ should contain at least one O star but that very massive clouds, $M \gtrsim 5 \times 10^5 M_\odot$, are likely ($P > 0.5$) to contain an association as luminous as Orion. Associations as luminous as the Rosette nebula are common only in the very most massive clouds, $M \gtrsim 2-3 \times 10^6 M_\odot$.

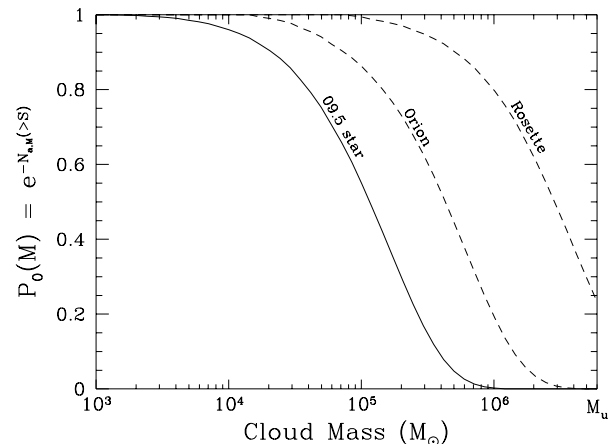


FIG. 7.—Probability, $P_0(M)$, that a cloud of mass M does not contain an O9.5 star. The generalization to associations of equal luminosity to the Orion and Rosette Nebulae is also shown.

4.4. The Most Luminous Association in a Cloud

By definition, for a small luminosity range, $\Delta \ln S$, the number of associations in the luminosity range S to $S(1 + \Delta \ln S)$ that are expected in a cloud of mass M is $\Delta \mathcal{N}_{a,M}(S) = d\mathcal{N}_{a,M}/d \ln S \cdot \Delta \ln S$. For sufficiently small $\Delta \ln S$, this is less than one and may be interpreted as a probability that there is an association with luminosity in the range $[S, S(1 + \Delta \ln S)]$ in the cloud.

We have also shown that $P_{0,S} = e^{-\mathcal{N}_{a,M}(>S)}$ is the probability that there are no associations more luminous than S in a cloud of mass M . Therefore, the probability that the most luminous association in the cloud is in the range ΔS about S is

$$P_{\max,S}(M) = \frac{d\mathcal{N}_{a,M}}{d \ln S} \Delta \ln S \cdot e^{-\mathcal{N}_{a,M}(>S)}. \quad (20)$$

This is graphed, again for an O9.5 star and the Orion and Rosette associations in Figure 8. For a cloud of mass $5 \times 10^5 M_\odot$, the probability that a single O9.5 star is the brightest association is small because such a cloud is expected to be forming more luminous associations. On the other hand, the Rosette is a very luminous association and is therefore rarely found in clouds of this mass. In fact, the most likely maximum luminosity association expected in such clouds is an Orion-type cluster, because it is common enough to be found in such clouds and is also fairly bright and therefore likely to be the brightest association in the cloud. A similar interpretation applies to other cloud masses.

4.5. Warm Clouds and Cold Clouds

To this point, we have treated the combination of the cloud mass and association luminosity functions, and the probability arguments that followed, under the assumption that any two clouds of equal mass have an equal propensity for forming stars (averaged over their lifetime). Yet, in § 3.2, it was shown that the cataloged clouds could account for only about 40% of the molecular mass in the first quadrant. Why should some clouds stand out (and be cataloged) and others not?

Solomon & Rivolo (1989) first introduced the idea of warm ($T_R^* > 7.5$ K) and cold ($T_R^* < 5$ K) clouds to explain this discrepancy, suggesting that the low CO temperatures

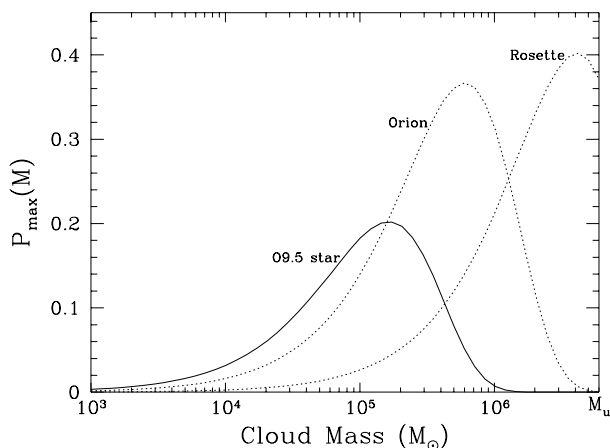


FIG. 8.—Probability, $P_{\max,S}(M)$, that an association with luminosity in the range $[S/2, 2S]$ is the brightest association in a cloud of mass M . As in Fig. 7, three graphs have been drawn at different values of S corresponding to an O9.5 star, and the Orion and Rosette Nebulae.

of the cold clouds would take on the appearance of a rather uniform background in the surveys and not be readily distinguishable as individual clouds. This is not necessarily inconsistent with our assumption if, for example, clouds spend part of their lifetime in a relatively quiescent phase without forming massive stars to heat their surroundings and produce high CO brightness temperatures (see McKee 1989). On the other hand, since the cold clouds are uncataloged and their properties are largely unknown, it may be that there are two (or more) completely distinct cloud populations, one star-forming, the other not. Since the definition of a “cold” cloud is somewhat arbitrary, however, one cannot simply identify the 60% of the clouds that are cold with clouds that are not forming stars. In any case, if only a fraction of the clouds are actively forming stars, the calculations presented in this section may be repeated for this subset of clouds by simply replacing the total mass of all molecular clouds by the mass of star-forming clouds in equation (16), resulting in greater association numbers per cloud, $\mathcal{N}_{a,M}(S)$, with a corresponding effect on the association luminosity probabilities. However, since \mathcal{N}_c is also lower, the total number of cloud-association pairs, $\mathcal{N}_a(S, M)$, is unchanged.

5. DISTRIBUTION OF STAR FORMATION EFFICIENCIES

Under the assumption that the locally derived IMF (Scalo 1986) applies throughout the Galaxy, the average star formation efficiency (SFE) per generation in Galactic molecular clouds is

$$\epsilon_T = 570 \left(\frac{0.75 S_{T,49}}{M_{\text{tot}}/M_\odot} \right) = 0.011 \quad (21)$$

from equation (10). Here we have assumed, based on the discussion at the beginning of § 4, that 75% of the total ionizing luminosity of the Galaxy ($S_{T,49} = 2.6 \times 10^4$ from Paper I) is emitted inside the solar circle. The typical efficiency can be considerably smaller than this, however: estimating the typical ionizing luminosity of the brightest association in a GMC of mass $3 \times 10^5 M_\odot$, for example, as $0.25 \times 10^{49} \text{ s}^{-1}$ from Figure 5, we find that the SFE due to that association is about 5×10^{-4} per generation. On the other hand, we have seen that the maximum SFE per generation is of order 0.1, which is considerably larger than the average. The SFE in molecular clouds thus ranges over 2 orders of magnitude, which raises the question of how the SFE is distributed in molecular clouds. We can address this question using the results that we have obtained on the joint distribution of OB associations and GMCs in the last section. In determining the SFE distribution, we must distinguish between the SFE of a single association in a cloud, ϵ , and the SFE of all the associations in a cloud, ϵ_M . We shall find the distribution of ϵ and the expected value of ϵ_M .

It should be kept in mind that a molecular cloud typically undergoes several generations of star formation; in Paper I, we adopted five generations as an average. With this value, the average SFE over the life of the association is about 0.05, and the maximum is about 0.5. The fact that the average SFE is so small, even when summed over generations, is consistent with the observation that most stars form in unbound associations (Miller & Scalo 1979).

The joint distribution in equation (16) is expressed in terms of the ionizing luminosity S . As shown in Paper I, the distribution of associations has a simple analytic form in

terms of the number of stars that have formed in one generation, \mathcal{N}_* ,

$$\frac{d\mathcal{N}_a(\mathcal{N}_*)}{d\ln \mathcal{N}_*} = \mathcal{N}_{au} \left(\frac{\mathcal{N}_{*u}}{\mathcal{N}_*} \right), \quad (22)$$

so it is convenient to write the joint distribution in terms of \mathcal{N}_* . Since \mathcal{N}_* is proportional to the expected value of S , we have $d\mathcal{N}_a(\mathcal{N}_*) = d\mathcal{N}_a(S)$, and the joint distribution (eq. [16]) becomes

$$\frac{d\mathcal{N}_{a,M}}{d\ln \mathcal{N}_*} = \frac{M}{M_{\text{tot}}} \cdot \frac{H[\mathcal{N}_{* \text{max}}(M) - \mathcal{N}_*]}{1 - (\mathcal{N}_*/b\mathcal{N}_{*u})^{1-\alpha}} \cdot \mathcal{N}_{au} \left(\frac{\mathcal{N}_{*u}}{\mathcal{N}_*} \right), \quad (23)$$

where the maximum number of stars in an association in a cloud of mass M is

$$\mathcal{N}_{* \text{max}} = \min [\mathcal{N}_{*u}, b(M/M_u)\mathcal{N}_{*u}] \quad (24)$$

from equation (13). For a cloud of a given mass, the probability that the SFE is in the range $d\epsilon$ is the same as the probability that the number of stars is in the range $d\mathcal{N}_*$, so that $d\mathcal{N}_{a,M}(\epsilon) = d\mathcal{N}_{a,M}(\mathcal{N}_*)$. Now the SFE for one generation of an association is

$$\epsilon = \frac{\mathcal{N}_* \bar{m}_*}{M}, \quad (25)$$

where \bar{m}_* is the average mass of a star in the IMF; for the Scalo (1986) IMF we adopted in Paper I, $\bar{m}_* = 0.51 M_\odot$. Thus the distribution of SFE's in clouds of mass M is

$$\frac{d\mathcal{N}_{a,M}(\epsilon)}{d\ln \epsilon} = \frac{M_u}{M_{\text{tot}}} \cdot \frac{H[\epsilon_{\text{max}}(M) - \epsilon]}{1 - (\epsilon M/b\epsilon_u M_u)^{1-\alpha}} \cdot \mathcal{N}_{au} \left(\frac{\epsilon_u}{\epsilon} \right). \quad (26)$$

Here $\epsilon_{\text{max}}(M)$ is ϵ_{max} for GMCs not near the upper mass limit M_u , but it is reduced to $\epsilon_u M_u/M$ for clouds with masses such that $M > M_u/b$. While it is quite possible that ϵ_{max} depends on M , our result for $\epsilon_{\text{max}}(M)$ is partly an artifact of the sharply truncated distributions of association luminosities and of cloud masses that we have adopted. It is likely that the data could be equally well fitted by assuming that $\epsilon_{\text{max}}(M)$ is constant but that the distributions deviate slightly from the assumed truncated power laws at large luminosities and masses, respectively.

Equation (26) shows that the number of associations in a cloud with an SFE of at least ϵ is about $(\mathcal{N}_{au} M_u/M_{\text{tot}})(\epsilon_u/\epsilon) \simeq 0.028(\epsilon_u/\epsilon)$. Only a few percent of clouds have an association with an SFE comparable to ϵ_u , and indeed only about 10% have an SFE that is greater than the average. Thus, star formation in the Galaxy is typically quite inefficient, but it is possible for the efficiency to increase by a factor of up to 100 on rare occasions.

Next, we determine the SFE summed over all the associations in a cloud of mass M . The expected value of the summed SFE is

$$\epsilon_M = \frac{1}{M} \int \mathcal{N}_* \bar{m}_* d\mathcal{N}_{a,M}(\mathcal{N}_*). \quad (27)$$

This integral can be evaluated analytically, with the result that

$$\frac{\epsilon_M}{\epsilon_T} = 1 + \frac{1}{\ln(\mathcal{N}_{*u}/\mathcal{N}_{*i})} \times \left\{ \ln \left(\frac{bM}{M_u} \right) - \frac{1}{1-\alpha} \ln \left[1 - \left(\frac{M}{M_u} \right)^{1-\alpha} \right] \right\}. \quad (28)$$

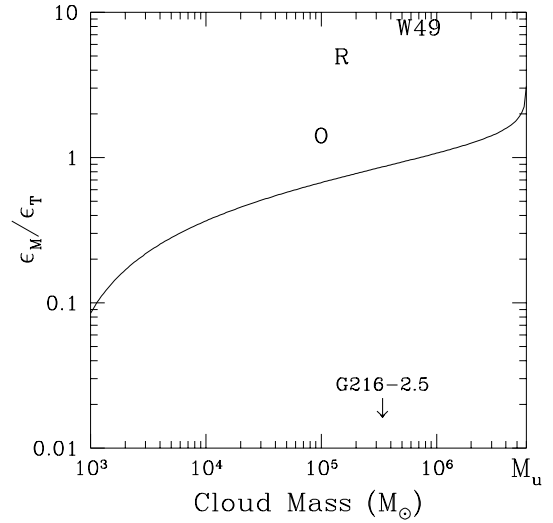


FIG. 9.—Overall ionizing star formation efficiency expected in a cloud as a function of its mass. $\epsilon_T = 0.011$ is the average ionizing star formation efficiency in the Galaxy. The efficiencies of W49, the Rosette, Orion, and G216-2.5 clouds are shown for comparison. The upper limit for G216-2.5 is based on the ionizing luminosity of a single O9.5 V star.

Figure 9 shows that the average of the summed SFE is less than the global average ϵ_T for low-mass clouds, since such clouds cannot contain large associations; to compensate for this, the average of the summed SFE is somewhat greater than ϵ_T for the most massive clouds.

6. GMC DESTRUCTION BY PHOTOEVAPORATION

6.1. Photoevaporation by a Single Association

An OB star, or an association of such stars, begins to destroy its natal molecular cloud as soon as it begins to emit ionizing radiation. The effective ionization lifetime of each generation of OB stars is $t_i \simeq 3.7 \times 10^6$ yr (Vacca et al. 1996). An OB association generally consists of several generations of OB star formation. Each generation of OB stars creates an H II region with an initial radius equal to the Strömgen radius in the molecular cloud, $R_{\text{St}} \simeq 0.6S_{49}^{1/3} n_{0,3}^{-2/3}$ pc, where $n_{0,3} \equiv n_0/(10^3 \text{ cm}^{-3})$ is the normalized initial density in the molecular cloud. Here we follow the notation of Paper I by denoting the total ionizing luminosity by S and that part of it that is absorbed by the gas (and not the dust) by S' ; on average, $S = 1.37S'$ in the Galaxy. The H II region will then expand, and it will usually break out into the ambient ISM, creating a “champagne flow” (Tenorio-Tagle 1979) or “blister H II region” (Icke 1979), as the ionized gas from the molecular cloud flows into the ambient medium.

Whitworth (1979) has developed a simple model for the blister stage of cloud photoevaporation. The pressure of the ionized gas in the H II region drives a shock front into the molecular cloud, creating a shell of compressed gas that expands away from the association (this shell of gas was not included in the analysis of Franco et al. 1994). An ionization front eats into the inner edge of the compressed shell. Now, the ram pressure of the shock advancing into the cloud, $\rho_0 v_s^2$, is comparable to the thermal pressure in the H II region, $\rho_i c_i^2$, where $c_i \simeq 10 \text{ km s}^{-1}$ is the isothermal sound speed in the H II region. It follows that the flux of ionized gas, $\sim \rho_i c_i$, is smaller than the flux of gas into the shock, $\rho_0 v_s$, by a factor v_s/c_i , which becomes smaller as the H II region expands. As a result, photoevaporation is an inher-

ently inefficient process: a single generation of OB stars in an association can generally ionize only a small fraction of its parent cloud. Whitworth (1979) estimated that an association would ionize a mass

$$\Delta M_i = 1930 n_{0,3}^{-1/7} S'_{49}{}^{4/7} t_6^{9/7} M_\odot \quad (29)$$

in a time t_6 Myr. The validity of this estimate has been confirmed in two-dimensional numerical calculations by Yorke et al. (1989). The characteristic size of the H II region in his model (denoted L by Whitworth) is

$$\ell = 8.7 n_{0,3}^{-2/7} S'_{49}{}^{1/7} t_6^{4/7} \text{ pc} . \quad (30)$$

In his model, the corresponding volume of the ionized region in the molecular cloud is $V_{\text{H II}} = \ell^3$.

If the association is sufficiently large or the cloud sufficiently small, the H II region will become comparable in size with the cloud. A substantial fraction of the cloud mass will have been swept up by the shock, so that the cloud is driven away from the association. In an early discussion of the effect of associations on molecular clouds, Elmegreen (1979) referred to this process as ‘‘cloud shuffling.’’ The H II region becomes comparable in size with the molecular cloud, $\ell = R$, where $R = 19.1(M_6/n_{0,3})^{1/3}$ pc, at a time t_R given by

$$t_{R,6} = 3.94 n_{0,3}^{-1/12} S'_{49}{}^{-1/4} M_6^{7/12} \text{ Myr} . \quad (31)$$

If t_R is less than the effective ionization lifetime ($t_i = 3.7 \times 10^6$ yr), the cloud will evolve toward the equilibrium cometary configuration studied by Bertoldi & McKee (1990). The transition to the cometary configuration is similar to the radiative implosion studied by Bertoldi (1989), but since the initial conditions differ from those he considered, it is difficult to make a quantitative estimate of the mass loss during this transition. The timescale for the transition is a shock crossing time and is therefore comparable to t_R . Since the cross-sectional area of the cometary cloud is significantly smaller than that of the initial cloud, and since the cloud is being driven away from the association, the mass-loss rate in the cometary stage of photoevaporation is much smaller than in the blister stage. As a result, we simply assume that the mass loss after the end of the blister stage can be approximated by extending Whitworth's estimate to a time $2t_R$. The total mass loss due to photoevaporation is then given by equation (29) with $t = \min(t_i, 2t_R)$:

$$\Delta M_i = \min [1.04 \times 10^4 n_{0,3}^{-1/7} S'_{49}{}^{4/7} , 2.7 \times 10^4 n_{0,3}^{-1/4} S'_{49}{}^{1/4} M_6^{3/4}] M_\odot . \quad (32)$$

The first case corresponds to associations that expire during the blister stage, whereas the second corresponds to associations that reach the cometary stage. The condition to enter the cometary stage is that $2t_R < t_i = 3.7 \times 10^6$ yr, corresponding to

$$S'_{49} > 20.6 n_{0,3}^{-1/3} M_6^{7/3} . \quad (33)$$

In both cases, we have assumed that the effective timescale for the photoevaporation is t_i . Small associations live longer than t_i , but the effectiveness of such associations in photoevaporating a cloud at late times is reduced both because larger associations can drive the cloud away and because the pressure of the cloud retards the ionization fronts of small associations at late times (see below).

The results for the photoevaporated mass depend weakly on the initial cloud density n_0 . As first shown by Larson (1981), GMCs tend to have a constant column density N_{H_2} ;

SRBY found a mean value of $170 M_\odot \text{ pc}^{-2}$, corresponding to $2N_{\text{H}_2} = 1.5 \times 10^{22} \text{ cm}^{-2}$ for Galactic GMCs. If desired, n_0 can be eliminated in favor of M and N_{H_2} by using

$$n_{0,3} = \frac{0.084}{M_6^{1/2}} \left(\frac{2N_{\text{H}_2}}{1.5 \times 10^{22} \text{ cm}^{-2}} \right)^{3/2} . \quad (34)$$

Before considering the effect of a collection of associations on a GMC, several comments are in order. First, it is important to keep in mind that there are two important assumptions that underlie the results we have taken from Whitworth (1979). The first assumption is that the pressure in the H II region is large enough to drive a shock into the surrounding GMC. Let $c_0 \equiv (P_0/\rho_0)^{1/2}$ be the effective sound speed in the GMC. The requirement that the shock velocity, which is about dl/dt , exceed c_0 for at least a time t_i restricts the mean density of the GMC to be

$$n_{0,3} < 36(S'_{49}{}^{1/2}/c_{0,5}^{7/2}) , \quad (35)$$

where $c_{0,5}$ is the effective sound speed in units of km s^{-1} . Typical GMCs in the Galaxy appear to have Alfvén velocities of $v_A \simeq 2 \text{ km s}^{-1}$ (Heiles et al. 1993), corresponding to $c_0 = (B^2/8\pi\rho)^{1/2} = v_A/2^{1/2} \simeq 1.4 \text{ km s}^{-1}$. The corresponding limit on the mean density of the GMC is $n_{0,3} \lesssim 10S'_{49}{}^{1/2}$, which is well satisfied by most Galactic GMCs; it may not be for GMCs in starburst galaxies, however. The shock may also become weak in the case of small H II regions, which have $S'_{49} \ll 1$ and lifetimes greater than the 3.7 Myr we have assumed in our numerical estimate. If the shock weakens, the photoevaporation rate will drop below the rate calculated by Whitworth.

The second assumption is that the velocity of the ionization front is less than the isothermal sound speed in the ionized gas, c_i , since otherwise the ionized gas cannot efficiently escape from the ionization front (Bertoldi 1989). As a result, the size of the H II region is limited to $\ell < c_i t_i = 35$ pc for our parameters. In view of this, very large GMCs can never reach the cometary stage of photoevaporation. In principle, this velocity limitation should be taken into account in determining the mass loss from the cloud, but the effect seems to be weak: the ratio of the mass loss given by equation (29) to that due to an ionization front advancing into the cloud at a velocity c_i is of order unity and scales very weakly with the ionizing luminosity.

Next, consider the maximum amount of photoevaporation due to a single generation of OB stars in an association. This can be found by setting S' equal to the maximum possible value it can have in a cloud of mass M , namely S'_{max} . From § 4 we find $S'_{\text{max},49} = 126M_6$, where we have used $S'_{u,49} = 360$ from Paper I. We can use either case in equation (32) to set an upper bound on the fraction of the cloud that is photoevaporated; the second case yields

$$\frac{\Delta M_i}{M} < 0.09 n_{0,3}^{-1/4} \rightarrow 0.17 M_6^{1/8} , \quad (36)$$

where the final expression is for a cloud with the typical column density found by SRBY. We conclude that an individual generation of OB stars in an association cannot photoevaporate a typical GMC.

If a single generation of OB stars cannot photoevaporate a typical GMC, what is the condition that it severely disrupt its parent cloud? A sufficient condition for severe disruption is for the photoevaporation to reach the cometary stage, which occurs if $S'_{49} > 47M_6^{5/2}$ from equations

(33) and (34). For example, the Rosette nebula has $S_{4.9} = 14$, which corresponds to $S'_{4.9} \simeq 10$ (Paper I); it will disrupt any cloud with $M < 6 \times 10^5 M_\odot$. Indeed, the Rosette nebula is a “blister” H II region that has blown away the surrounding molecular material and has strongly affected the remainder of the cloud (Williams et al. 1995). However, reference to Figure 5 shows that typically there is only a small chance that a cloud of that mass will have an association as luminous as the Rosette, so we infer that massive GMCs ($M \gtrsim 10^6 M_\odot$) are rarely completely disrupted by a single generation of OB stars. On the other hand, a single O9.5 star, which has $S_{4.9} = 0.24$, corresponding to $S'_{4.9} = 0.18$, will completely disrupt any cloud with $M \lesssim 10^5 M_\odot$. It is far more common that clouds of such mass contain at least one O star, and therefore will be severely disrupted. The Orion molecular cloud, for example, has been severely disrupted by a small association consisting of only three O stars (Bally et al. 1987).

Finally, we note that there is a direct connection between the picture of cloud photoevaporation we have described here and the H II envelopes described in Paper I. There we concluded that about $\frac{2}{3}$ of the ionizing photons escaped from the immediate vicinity of an association (the radio H II region) and were absorbed in a surrounding H II envelope. In Whitworth’s (1979) model for a blister H II region, somewhat less than half the ionizing photons escape into the envelope, but this fraction is increased for H II regions that can evolve for a time $t_i \gtrsim t_R$. For cometary H II regions, most of the ionizing photons can escape. As we have seen, however, cometary H II regions predominate only in smaller GMCs, which contain only a small fraction of the total ionizing luminosity of the Galaxy. We thus expect a typical H II region to have comparable numbers of ionizing photons absorbed in the local GMC and in the ambient envelope, which is consistent with the model adopted in Paper I.

6.2. GMC Lifetimes

We can now use the results of § 4 to determine the net photoevaporation rate due to all the associations in a GMC. The expected number of associations with ionizing luminosities between S and $S + dS$ in a given cloud of mass M is $d\mathcal{N}_{a,M}(S)$. Since the effective lifetime of each generation is t_i , their birthrate is $d\mathcal{N}_{a,M}(S)/t_i$. Each generation of an association photoevaporates a mass ΔM_i . In the absence of interaction among the H II regions, the net rate of photoevaporation is

$$\dot{M}_i = \frac{1}{t_i} \int \Delta M_i(S) d\mathcal{N}_{a,M}(S). \quad (37)$$

The corresponding cloud destruction time is

$$t_{d0} = M/\dot{M}_i. \quad (38)$$

This result is graphed in Figure 10. The actual cloud destruction time t_d , allowing for interactions among the H II regions, will be estimated below. The treatment of photoevaporation during the transition from the blister stage to the cometary stage is quite approximate, which renders our estimate of t_{d0} for the smaller clouds correspondingly uncertain. It would be worthwhile to study the late evolution of photoevaporating clouds more carefully, both observationally (see, e.g., Leisawitz 1990; Williams & Maddalena 1996) and theoretically.

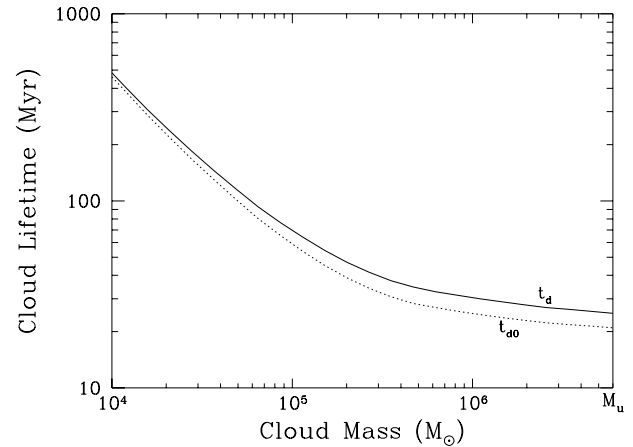


FIG. 10.—Destruction timescale for cloud photoevaporation based on the expected number of associations in a cloud (Fig. 5). The dotted line is the calculated lifetime, t_{d0} , without the effect of multiple overlapping associations (porosity) taken into account. The solid line, t_d , includes the effect of association porosity. Photoevaporation is most effective for clouds with masses $M \gtrsim 10^5 M_\odot$, for which lifetimes $t_d \simeq 30$ –40 Myr are inferred. Photoevaporation operates on an increasingly longer timescale for lower mass clouds, which are not expected to form large numbers of O stars.

An important feature of cloud destruction by photoevaporation is that it is dominated by relatively small H II regions. The median luminosity for cloud destruction, such that half the cloud photoevaporation is due to lower luminosity associations and half to brighter associations, is $S_{\text{median},4.9} = 3.7$ for $M > 10^5 M_\odot$. This is surprisingly small (an Orion-type association) and demonstrates that the combined effects of large numbers of small associations are very effective at destroying even the largest clouds.

The rapid increase of t_{d0} for clouds of mass $M \lesssim 2 \times 10^5 M_\odot$ represents the decreasing role of photoionization in the destruction of these clouds. Such clouds are small enough that individual O stars can drive the clouds past the blister stage and into the cometary stage of photoevaporation, so that the mass-loss rate saturates at the value given by the second expression in equation (32). The lifetime of these smaller clouds may nonetheless be governed indirectly by photoevaporation: since this process is so disruptive for small clouds, they may be fragmented into sufficiently small pieces that they are converted into atomic form by photo-dissociation. On the other hand, the lifetime of some of the small clouds may be determined by the reverse process of agglomeration into larger complexes.

Additional insight on cloud destruction can be obtained from analytic estimates. As mentioned above, the destruction is dominated by relatively small H II regions with $S \ll S_u$. The actual luminosity function for H II regions is complicated (see Paper I), but for simplicity we shall extrapolate the approximate luminosity function given in equation (9) down to a lower cutoff S_l . In Paper I, we found that a power law with $S_{l,4.9} \simeq 0.1$ gives the correct total ionizing luminosity. Here, however, we wish to choose a lower cutoff that gives the correct rate of cloud destruction, and we find that $S_{l,4.9} = 0.14$ gives a better fit to our numerical results. We thus approximate the joint distribution given in equation (16) by

$$\frac{d\mathcal{N}_{a,M}(S)}{d \ln S} \simeq \frac{M}{M_{\text{tot}}} \cdot \mathcal{N}_{au} \frac{S_u}{S}, \quad (0.14 \times 10^{49} \text{ s}^{-1} < S \ll S_{\text{max}}). \quad (39)$$

With this approximation for the joint distribution of clouds and associations, we can use equations (32) and (37) to evaluate the cloud destruction time for blister H II regions (Case 1) as

$$t_{d0,1} \simeq \frac{24}{M_6^{1/14}} \left(\frac{2N_{\text{H}_2}}{1.5 \times 10^{22} \text{ cm}^{-2}} \right)^{3/14} \text{ Myr}, \quad (40)$$

whereas for associations that reach the cometary stage (Case 2) we have

$$t_{d0,2} \simeq \frac{6.1}{M_6^{7/8}} \left(\frac{2N_{\text{H}_2}}{1.5 \times 10^{22} \text{ cm}^{-2}} \right)^{3/8} \text{ Myr}. \quad (41)$$

The first expression is appropriate for massive clouds, whereas the second is appropriate for small clouds. An approximation valid for all clouds can be obtained by simply summing the two expressions, $t_{d0} \simeq t_{d0,1} + t_{d0,2}$. As remarked above, however, the actual cloud destruction time t_d is somewhat larger than this due to interaction among the H II regions, and we turn to this issue now.

6.3. Porosity of H II Regions

In describing the filling factor of the hot gas in the diffuse ISM, Cox & Smith (1974) introduced the concept of the porosity of the hot gas, $Q = (\text{SN rate}) \int V(t) dt$, where $V(t)$ is the volume of a supernova remnant of age t . The porosity is related to the filling factor of the SNRs in spacetime (McKee 1990), which is equivalent to the time average of the spatial filling factor; for small Q , the porosity and the filling factor are about the same. Just as the porosity of SNRs in the ISM can determine the structure of the ISM, so too the porosity of H II regions in a GMC can determine the structure and evolution of the GMC. If Q is small, then the H II regions would have little effect on the GMC. However, if the formation of massive stars is self-regulating, as in the Elmegreen & Lada (1977) model, then one might expect $Q \sim 1$. Furthermore, in this case the interaction among the H II regions can affect the destruction time for the clouds.

Let $V_{\text{H II}}(S, t)$ be the volume in a GMC occupied by an H II region of age t and ionizing luminosity S . For blister H II regions (the first of the cases considered in eq. [32]), this volume is simply $[l(t)]^3$, whereas for cometary H II regions we set $V_{\text{H II}}(S, t) = [l(2t_R)]^3 = 2^{12/7} R^3 \simeq 0.8 V_{\text{cl}}$, where V_{cl} is the volume of the GMC. Note that this volume is defined with respect to the location of the cloud at the time the association turns on; by the time we observe the association and the cloud, the cloud may have already been displaced from the association, just as the Orion molecular cloud has moved away from the associations in Orion that are older than the Trapezium. The porosity of H II regions in the cloud is then

$$Q = \frac{1}{V_{\text{cl}} t_i} \int d\mathcal{N}_{a,M}(S) \int V_{\text{H II}}(S, t) dt. \quad (42)$$

The porosity is portrayed in Figure 11 using the luminosity function of OB associations found in Paper I. The fact that Q is of order unity for massive clouds suggests that the rate of massive star formation is self-regulated. Just as in the case of the cloud destruction time, the porosity is dominated by relatively small H II regions.

We can obtain an analytic estimate of Q by using the same approximation for the joint distribution of clouds and associations that we used to estimate the cloud destruction

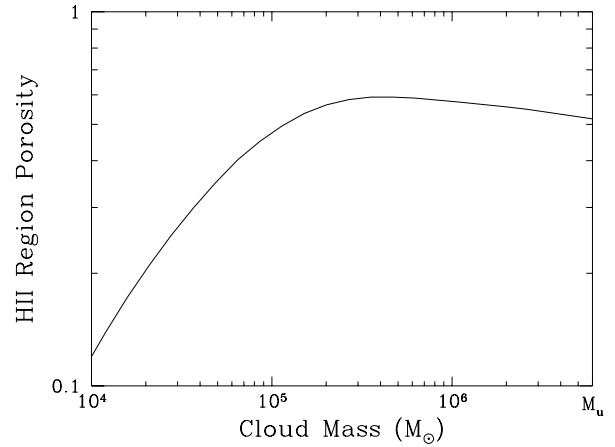


FIG. 11.—Expected H II region porosity, Q , as a function of cloud mass. For low-mass clouds, OB associations are rare and the filling factor of their H II regions is small. For high-mass clouds, there can be significant overlap among H II regions.

time. For blister H II regions (the first case in eq. [32], appropriate for massive clouds), we find

$$Q_1 \simeq \frac{0.59}{M_6^{1/14}} \left(\frac{2N_{\text{H}_2}}{1.5 \times 10^{22} \text{ cm}^{-2}} \right)^{3/14}, \quad (43)$$

whereas for H II regions that have reached the cometary stage (appropriate for low-mass clouds), we find

$$Q_2 \simeq 12.7 M_6. \quad (44)$$

The porosity in intermediate cases can be estimated to within 10% of the true value by the harmonic mean of these two expressions, $Q^{-1} = Q_1^{-1} + Q_2^{-1}$.

If the porosity is of order unity, interactions among the H II regions will affect the filling factor of the ionized gas in the GMC. Q may be regarded as the expected number of other associations in a given H II region. In effect, the number of associations is reduced by a factor $1 + Q$, and the luminosity of each association is increased by the same factor. For massive clouds, which have the largest porosity, the destruction is dominated by blister H II regions with $\Delta M_i \propto S^{4/7}$. As a result, the cloud destruction time corrected for the interaction among H II regions, t_d , is given by

$$\frac{M}{t_d} = \frac{1}{t_i} \int (1 + Q)^{4/7} \Delta M_i \cdot \frac{d\mathcal{N}_{a,M}(S)}{(1 + Q)}, \quad (45)$$

so that

$$t_d = (1 + Q)^{3/7} t_{d0}. \quad (46)$$

Our result for the cloud destruction time, t_d , is graphed in Figure 10. It shows that star-forming GMCs with $M \gtrsim 5 \times 10^5 M_\odot$ have a lifetime ~ 30 – 40 Myr, almost independent of mass, in agreement with a number of other estimates (Bash, Green, & Peters 1977; Blitz & Shu 1980; Leisawitz 1990). This lifetime is also consistent with the model for the evolution of an OB association we adopted in Paper I, in which each association typically goes through about five generations of star formation over a time $5t_i = 18.5$ Myr; a massive cloud has a relatively luminous association for about half its life. Less massive clouds are not destroyed by photoionization, but they are severely disrupted; as a result, the destruction time t_d is likely to be much greater than the lifetime of the cloud as a coherent entity.

Finally, we note that if only some GMCs are forming stars, as discussed in § 4.5, then the lifetime of the star-forming clouds will be correspondingly decreased, and the porosity of the H II regions will be increased. However, since the smaller associations dominate the cloud destruction, it is quite possible that some of the cold clouds that escaped being cataloged by Solomon et al. (1987) are in fact in the process of being destroyed by photoevaporation.

6.4. Photoionization Rate of GMCs in the Galaxy

The total rate of photoionization of GMCs in the inner part of the Galaxy ($R < 8.5$ kpc) is simply

$$\dot{M}_i(\text{Galaxy}) = \int \frac{M}{t_d} d\mathcal{N}_c(M). \quad (47)$$

Numerical evaluation of this integral gives a total ionization rate of $27 M_\odot \text{ yr}^{-1}$. Insofar as H II regions primarily ionize the molecular gas in GMCs rather than their atomic envelopes, this is approximately the rate at which molecular gas is ionized in the Galaxy. The corresponding harmonic mean destruction time is $\langle t_d \rangle = 10^9 M_\odot / (27 M_\odot \text{ yr}^{-1}) = 37$ Myr. Since the star formation rate in the inner part of the Galaxy is about $\frac{3}{4}$ of the total rate of $4 M_\odot \text{ yr}^{-1}$ estimated in Paper I, it follows that $\sim 9 M_\odot$ of gas is photoionized for each solar mass of stars formed. The fraction of a GMC that would be converted into stars before it is destroyed—i.e., the star formation efficiency over the lifetime of the cloud—is therefore about 10%. Whitworth (1979) estimated that O stars would destroy a cloud after only 4% of its mass was converted to stars, but he did not allow for the possibility that H II regions could evolve from the blister stage to the cometary stage.

The integrated star formation efficiency we have estimated here is twice what we found in § 5, since the time it takes to photoevaporate a cloud is about twice the estimated 20 Myr lifetime of an association (Blaauw 1991). That is, the two SFEs are different: in § 5, we determined the SFE over the life of an association, whereas here we have determined it over the life of a cloud. In view of the uncertainties in calculating the destruction rate due to photoevaporation, it is possible that we have underestimated the rate by a factor 2. If the discrepancy is real, however, there are two main possibilities. One is to assume that cloud disruption is comparable to cloud destruction in limiting the lifetime of an association, so that the cloud lifetime is about twice the lifetime of an association. In this picture, during its 20 Myr life, an association would so disperse its natal cloud that the subsequent star formation in that molecular gas would not be attributed to the original association. Alternatively, as discussed in § 4.5, not all clouds may actively form OB stars. For example, in the theory of photoionization-regulated star formation (McKee 1989), about half of all GMCs have a relatively low column density and cannot form stars efficiently, whereas the other half have contracted to a sufficiently high column density that they can form stars efficiently. If only half of the clouds were star forming, then $\mathcal{N}_{a,M}$ for these clouds would be twice as large, t_{d0} half as large, and the porosity twice as high. As a result, the actual destruction time, t_d , would be somewhat less than a factor of 2 shorter. For an equal proportion of star-forming and non-star-forming clouds, we find $\dot{M}_i(\text{Galaxy}) = 24 M_\odot \text{ yr}^{-1}$. This is about the same rate as that found above for the case in which all the clouds are star forming, so again about 10% of a cloud is turned into stars before the cloud is

destroyed. The harmonic mean cloud lifetime, $\langle t_d \rangle = 0.5 \times 10^9 M_\odot / (24 M_\odot \text{ yr}^{-1}) = 21$ Myr, is then comparable to the observed lifetime of associations.

7. SUMMARY

There are two main parts to this paper. The first is a new estimate for the mass spectrum of molecular clouds in the Galaxy, and the second is the combination of this result with the luminosity distribution of OB associations in the Galaxy that we derived in Paper I.

For the first part, we used four cloud catalogs: three of the first quadrant (DECT, SRBY and SYCSW), and one of the solar neighborhood (Dame et al. 1986). There were a number of steps involved which we summarize here:

1. Cloud masses from the different catalogs were adjusted to a uniform set of parameters (X, α_{vir} ; Table 1). Clouds for which the distance ambiguity was not resolved were rejected from further analysis.
2. Clouds were binned by mass and the number per bin fit to a truncated power law.
3. The fit was extrapolated to lower masses, and from the area of the CO surveys to the inner Galaxy, $0.2R_0 < R < R_0$. The total cloud mass was found to be a factor of 2.5 less than the total mass of molecular gas measured in the inner Galaxy by Bronfman et al. (1988). This discrepancy implied that the observed cloud distribution does not fully represent the true distribution and two models representing two extreme possibilities were adopted: a uniform scaling of the observed distribution (Model A), and a steeper distribution than observed (Model B).
4. The predictions of each model for the number of clouds in the solar neighborhood ($d < 1$ kpc) were compared to the observations, assuming that the radial dependence of cloud numbers declined exponentially with a scale length, $H_R = 3.5$ kpc (measured from the decrease in molecular gas surface density). The predictions were found to be within a factor of 2 of the actual numbers of clouds, and the gradual falloff in number with mass favored Model A over Model B.

The mass spectrum that we find as a result of this analysis is, therefore, consistent with the catalogs of the first quadrant, the distribution of clouds in the solar neighborhood, and the total molecular mass in the Galaxy. Its differential form is

$$\frac{d\mathcal{N}_c}{d \ln M} = 63 \left(\frac{6 \times 10^6 M_\odot}{M} \right)^{0.6},$$

$$(M \leq 6 \times 10^6 M_\odot, 1.7 \text{ kpc} \leq R \leq 8.5 \text{ kpc}),$$

which gives a total molecular mass between 1.7 kpc and 8.5 kpc of

$$M_{\text{tot}} = \mathcal{N}_{cu} M_u / (1 - \alpha) = 1.0 \times 10^9 M_\odot.$$

Cloud masses are determined by formation mechanisms but may subsequently evolve through the effects of collisional agglomeration, tidal shear, and stellar destruction. The manner in which the molecular material in the Galaxy is divided up into clouds and cloud complexes must reflect the behavior of these competing processes. A significant difference between our analysis and that of previous work is the explicit inclusion of an upper limit to the mass spectrum, M_u . The need for such a cutoff can be seen in the catalogs, even though they account for only 40% of the emission in the CO surveys, and is confirmed by the Grabelsky et al.

(1988) study of the Carina arm: there are no observations of clouds with masses in excess of $\sim 6 \times 10^6 M_\odot$ (other than very massive blended objects in the SYCSW catalog that are not believed to be clouds). Since there are substantial numbers of clouds at or near this maximum mass, there must be some effective formation limit or destructive process that prevents clouds from exceeding this limit.

The second half of the paper concerned itself with the allocation of OB associations into GMCs. Having determined the number of OB associations in Paper I and the number of molecular clouds in the first half of this paper, we determined the average number of OB associations per cloud. Because there is a range of luminosities of associations and of masses of clouds, this basic question became one of determining the distribution of associations of luminosity S in a cloud of mass M . The one constraint on this joint distribution is that the overall number of associations of luminosity S summed over all clouds must equal the total number of associations in the Galaxy, i.e., the joint distribution integrated over the mass spectrum must equal the luminosity distribution. Even with this constraint, the allocation of associations in clouds is not uniquely determined and one must make a number of assumptions before proceeding.

We chose as minimal a set of assumptions as seems possible. They were motivated by two physical ideas:

1. The star formation efficiency of an association in a cloud, ϵ , is limited to be less than a fixed maximum value, ϵ_{\max} .
2. The star formation rate per unit mass of gas is constant, to the extent that this is consistent with (1).

The first assumption can be restated as being a limit on the luminosity of the brightest association in a cloud, $S \leq S_{\max}(M)$. The second is equivalent to stating that the number of associations of each luminosity S in a cloud of mass M is half that expected in a cloud of mass $2M$, subject to the above proviso that this number drops to zero if $S > S_{\max}(M)$. These two conditions plus the integral constraint defined the joint distribution uniquely. Using this as a starting point and assuming Poisson statistics for the distribution of OB associations about the mean, we were able to determine the probability that a cloud be devoid of O stars. For clouds of mass $10^5 M_\odot$, about half are expected to contain at least one OB star or association, and about half not. We also determined a distribution for the brightest association per cloud and the total number of cloud-association pairs in the Galaxy.

OB associations ionize and disrupt their molecular surroundings, thereby limiting a cloud's lifetime. Using estimates of the destructive effect of an association on a cloud and our determination of the expected number of such associations per cloud, we have determined the photoevaporative timescale for clouds of different mass. High-mass clouds, $M \gtrsim 3 \times 10^5 M_\odot$, are predominantly destroyed by large numbers of small associations that form blister H II regions in a time $\sim 30\text{--}40$ Myr. H II regions in low-mass clouds, $M \lesssim 10^5 M_\odot$, can often evolve beyond the blister

stage into the cometary stage of photoevaporation. As a result, small clouds are disrupted by O stars, rather than being photoionized. The number of ionizing photons that escape from the GMC increases as an H II region evolves, so that most of the photons escape from cometary H II regions. For the more massive GMCs, which are the source of most of the ionizing luminosity of the Galaxy, most associations never reach the cometary stage, and as a result comparable numbers of ionizing photons are absorbed locally and in the surrounding H II envelope. We estimated the porosity Q of the H II regions in a molecular cloud, which roughly speaking is the fraction of the original volume of the molecular cloud occupied by H II regions. For massive clouds, we found that Q is of order (but somewhat less than) unity, which is consistent with the idea that the rate of massive star formation is self-regulated by some process.

The average star formation efficiency over the life of an association is 5%. Our models show that this may vary by more than 2 orders of magnitude from cloud to cloud but is predicted to increase with cloud mass. Clouds of mass $\approx 10^6 M_\odot$ have an expected efficiency equal to the Galactic average, and thus about half (by mass) of the clouds form stars at greater than average efficiency, and half less.

On the other hand, our results on cloud photoevaporation show that the star formation efficiency over the life of a cloud is 10%. If this difference in the efficiencies is real and is not an artifact of our model, it can be accounted for by assuming that only about half of all GMCs are actively forming stars. In that case, the lifetime of a star-forming cloud becomes comparable to the observed lifetime of associations, about 20 Myr.

Implicit in our assumptions is that of cloud equality: one cloud of mass M is exactly the same as another of mass M (or at least one star-forming cloud is the same as another star-forming cloud of the same mass). There is no time dependence in our joint distribution, so we cannot treat age or evolutionary differences between clouds, nor have we allowed for differences in the cloud environments. The treatment here has been deliberately chosen to be the simplest possible that is consistent with the available data. Nonetheless, our results demonstrate once again that star formation in the Galaxy is a relatively inefficient process: there is too much molecular material and there are too few associations to make every cloud an Orion or a Rosette, and correspondingly there are substantial molecular clouds with very few ionizing stars.

J. P. W. thanks the Harvard-Smithsonian Center for Astrophysics for fellowship support. The research of C. F. M. is supported in part by NSF grants AST92-21289 and AST95-30480 and, for research in star formation, by a grant from the NASA Astrophysical Theory Program. We would like to thank Tom Dame, Nick Scoville, and Phil Solomon for making their cloud catalogs available in electronic form, and for their advice concerning them. Conversations with Jan Brand, Matt Richter, Pat Thaddeus, and Jack Welch are also appreciated.

REFERENCES

- Adler, D. S., & Roberts, W. W. 1992, *ApJ*, 384, 95
 Anantharamaiah, K. R. 1985, *J. Astr. Ap.*, 6, 203
 Bahcall, J. N., & Soneira, R. M. 1980, *ApJS*, 44, 73
 Bally, J., Langer, W. D., Stark, A. A., & Wilson, R. W. 1987, *ApJ*, 312, L45
 Bash, F. N., Green, E., & Peters, W. L., III. 1977, *ApJ*, 217, 464
 Bertoldi, F. 1989, *ApJ*, 346, 735
 Bertoldi, F., & McKee, C. F. 1990, *ApJ*, 354, 529
 ———. 1992, *ApJ*, 395, 140
 Blaauw, A. 1991, in *The Physics of Star Formation and Early Stellar Evolution*, ed. C. Lada & N. Kylafis (Dordrecht: Kluwer), 125
 Blitz, L., & Shu, F. H. 1980, *ApJ*, 238, 148
 Blitz, L., & Thaddeus, P. 1980, *ApJ*, 241, 676

- Bronfman, L., Cohen, R. S., Alvarez, H., May, J., & Thaddeus, P. 1988, *ApJ*, 324, 248
- Brand, J., & Wouterloot, J. G. A. 1995, *A&A*, 303, 851
- Cardelli, J. A., & Clayton, G. C. 1988, *AJ*, 95, 516
- Carpenter, J. 1994, Ph.D. thesis, Univ. of Massachusetts
- Carpenter, J. M., Snell, R. L., & Schloerb, F. P. 1990, *ApJ*, 362, 147
- Cohen, R. S., Dame, T. M., & Thaddeus, P. 1986, *ApJS*, 60, 695
- Cox, D. P., & Smith, B. W. 1974, *ApJ*, 189, L105
- Cox, P., Deharveng, L., & Leene, A. 1991, *A&A*, 230, 171
- Dame, T. M. 1993, in *Back to the Galaxy*, ed. S. S. Holt & F. Verter (New York: AIP), 267
- . 1995, private communication
- Dame, T. M., Elmegreen, B. G., Cohen, R. S., & Thaddeus, P. 1986, *ApJ*, 305, 892 (DECT)
- Dame, T. M., & Thaddeus, P. 1985, *ApJ*, 297, 751
- Dame, T. M., Ungerechts, H., Cohen, R. S., de Geus, E. J., Grenier, I. A., May, J., Murphy, D. C., Nyman, L.-Å., & Thaddeus, P. 1987, *ApJ*, 322, 706
- Dickey, J. M., & Garwood, R. W. 1989, *ApJ*, 341, 201
- Digel, S., Bally, J., & Thaddeus, P. 1990, *ApJ*, 357, L29
- Digel, S., de Geus, E., & Thaddeus, P. 1994, *ApJ*, 422, 92
- Elmegreen, B. G. 1979, *ApJ*, 2231, 372
- Elmegreen, B. G., & Clemens, C. 1985, *ApJ*, 294, 523
- Elmegreen, B. G., & Lada, C. J. 1977, *ApJ*, 214, 725
- Franco, J., Shore, S. N., & Tenorio-Tagle, G. 1994, *ApJ*, 436, 795
- Grabelsky, D. A., Cohen, R. S., Bronfman, L., & Thaddeus, P. 1988, *ApJ*, 331, 181
- Gwinn, C. R., Moran, J. M., & Reid, M. J. 1992, *ApJ*, 393, 149
- Heiles, C., Goodman, A. A., McKee, C. F., & Zweibel, E. 1993, in *Protostars and Planets III*, ed. E. H. Levy & J. I. Lunine (Tucson: Univ. of Arizona Press), 279
- Heiles, C., Reach, W. T., & Koo, B.-C. 1996, *ApJ*, 466, 191
- Icke, V. 1979, *A&A*, 78, 352
- Kenyon, S. J., Hartmann, L. W., Strom, K. M., & Strom, S. E. 1990, *AJ*, 99, 869
- Lacey, C. G., & Fall, S. M. 1985, *ApJ*, 290, 154
- Lada, C. J., & Wilking, B. A. 1984, *ApJ*, 287, 610
- Larson, R. B. 1981, *MNRAS*, 194, 809
- Leisawitz, D. 1990, *ApJ*, 359, 319
- Maddalena, R. J., Morris, M., Moscovitz, J., & Thaddeus, P. 1986, *ApJ*, 303, 375
- Maddalena, R. J., & Thaddeus, P. 1985, *ApJ*, 294, 231
- McKee, C. F. 1989, *ApJ*, 345, 782
- . 1990, in *ASP Conf. Proc. 12, The Evolution of the Interstellar Medium*, ed. L. Blitz (San Francisco: ASP), 3
- McKee, C. F., Van Buren, D., & Lazareff, B. 1984, *ApJ*, 278, L115
- McKee, C. F., & Williams, J. P. 1997, *ApJ*, 476, 144 (Paper I)
- Miller, G. E., & Scalo, J. M. 1979, *ApJS*, 41, 513
- Mooney, T. J., & Solomon, P. M. 1988, *ApJ*, 334, L51
- Myers, P. C., Dame, T. M., Thaddeus, P., Cohen, R. S., Silverberg, R. F., Dwek, E., & Hauser, M. G. 1986, *ApJ*, 301, 398
- Sanders, D. B., Clemens, D. P., Scoville, N. Z., & Solomon, P. M. 1986, *ApJS*, 60, 1
- Scalo, J. 1986, *Fundam. Cosmic Phys.*, 11, 1
- Scoville, N. Z., & Good, J. C. 1989, *ApJ*, 339, 149
- Scoville, N. Z., Yun, M. S., Clemens, D. P., Sanders, D. B., & Waller, W. H. 1987, *ApJS*, 63, 821 (SYCSW)
- Smith, L. F., Biermann, P., & Mezger, P. G. 1978, *A&A*, 66, 65
- Sodroski, T. J., et al. 1995, *ApJ*, 452, 262
- Solomon, P. M., & Rivolo, A. R. 1989, *ApJ*, 339, 919
- Solomon, P. M., Rivolo, A. R., Barrett, J., & Yahil, A. 1987, *ApJ*, 319, 730 (SRBY)
- Strong, A. W., et al. 1997, in preparation
- Taylor, J. H., & Cordes, J. M. 1993, *ApJ*, 411, 674
- Tenorio-Tagle, G. 1979, *A&A*, 71, 59
- Vacca, W. D., Garmany, C. D., & Shull, J. M. 1996, *ApJ*, 460, 914
- Ward-Thompson, D., & Robson, E. I. 1990, *MNRAS*, 244, 458
- Whitworth, A. 1979, *MNRAS*, 186, 59
- Williams, J. P., Blitz, L., & Stark, A. A. 1995, *ApJ*, 451, 252
- Williams, J. P., de Geus, E. J., & Blitz, L. 1994, *ApJ*, 428, 693
- Williams, J. P., & Maddalena, R. J. 1996, *ApJ*, 464, 247
- Wouterloot, J. G. A., Brand, J., Burton, W. B., & Kwee, K. K. 1990, *A&A*, 230, 21
- Yorke, H. W., Tenorio-Tagle, G., Bodenheimer, P., & Rozyczka, M. 1989, *A&A*, 216, 207